

Exorcising Ghosts in Induced Gravity

Gaurav Narain*

*Kavli Institute for Theoretical Physics China (KITPC),
Key Laboratory of Theoretical Physics,
Institute of Theoretical Physics (ITP),
Chinese Academy of Sciences (CAS), Beijing 100190, P.R. China.*

Abstract

Unitarity of scale-invariant coupled theory of higher-derivative gravity and matter is investigated. A scalar field coupled with Dirac fermion is taken as matter sector. Following the idea of induced gravity Einstein-Hilbert term is generated via dynamical symmetry breaking of scale-invariance. The renormalisation group flows are computed and one-loop RG improved effective potential of scalar is calculated. Scalar field develops a new minimum via Coleman-Weinberg procedure inducing Newton's constant and masses in the matter sector. The spin-2 problematic ghost and the spin-0 mode of the metric fluctuation gets a mass in the broken phase of theory. The energy-dependence of VeV in the RG improved scenario implies a running for the induced parameters. This sets up platform to ask whether it is possible to evade the spin-2 ghost by keeping its mass always above the running energy scale? In broken phase this question is satisfactorily answered for a large domain of coupling parameter space where the ghost is evaded. The spin-0 mode can be made physically realisable or not depending upon the choice of initial parameters. Induced Newton's constant is seen to vanish in ultraviolet. By properly choosing parameters it is possible to make the matter fields physically unrealisable.

arXiv:1612.04930v2 [hep-th] 20 Oct 2017

*Electronic address: gaunarain@itp.ac.cn

I. INTRODUCTION

Finding a well-defined and mathematically consistent theory of quantum gravity is one of the most important problems of theoretical physics. Moreover, finding experimental evidence validating or falsifying one is equally hard. Presently there are several models of quantum gravity which are aimed at studying the quantum nature of space-time and investigating physics at ultra-high energies. Recently a minimalistic model in the framework of four dimension quantum field theory (QFT) in lorentzian space-time was investigated, which was shown to be renormalizable to all loops [1, 2], and was recently shown to be unitary [5, 6] (see also references therein). This then offers a sufficiently good and simple model of quantum field theory of gravity whose arena can be used to investigate physics at ultra-high energies.

Here in this paper, motivated by the results of [2–8] we study the scale-invariant higher-derivative gravitational system coupled with matter fields. These constitute interesting systems. The scale-invariant purely gravitational sector consist of only dimensionless couplings. This makes the theory perturbatively renormalizable to all loops in four space-time dimensions by power-counting [9, 10] (for classical picture of these theories see [1, 11]). Coupling this with scale-invariant matter sector doesn't change the picture. The resulting theory is still perturbatively UV renormalizable in four dimensions due to lack of any dimensionful parameter. Classically the matter sector however has local conformal invariance, which is broken under quantum corrections due to conformal anomalies (local and non-local) [12, 13]. The interesting thing to note here is that in this quantum theory the counter terms generated still possess scale invariant structure (due to lack of any dimensionful parameter in theory) [14]. This therefore preserves the renormalizability of theory [2], even though trace anomalies are present.

Scale-invariant gravitational systems coupled with matter have been investigated in past. Some of the first studies were conducted in [4, 9, 10, 15, 16], where the renormalisation group running of various couplings was computed and fixed point structure was analysed. Further investigation for more complicated systems were done in [17–22] (see also the book [23]). Matter coupling with conformal quantum gravity along with Gauss-Bonnet term were investigated in [24, 25]. Recently it has gained some momentum and these models have been reinvestigated [26, 30–33]. The purpose in these papers were to see if it is possible to generate a scale dynamically starting from scale-invariant system. In [26] the authors called their model ‘Agravity’, where Planck scale is dynamically generated from the vacuum-expectation-value (VeV) of potential in Einstein frame (not in Jordan frame). By this they achieve a negligible cosmological constant, generates Planck’s mass, and addresses the naturalness [26, 27] and inflation [28], but unitarity issues was not explored ¹. In [30–33] the authors studies the issue of dynamical generation of scale via dimensional transmutation in the presence of background curvature. This also induces Einstein-Hilbert gravity and generates Newton’s constant, but unitarity problem was not addressed. An interesting idea has been suggested in [34, 35] by assuming an analogy with QCD, where the authors addresses the problems of ghost and tachyon using the wisdom acquired from non-perturbative sector of QCD, as is argued that the gravitational theory enters a non-perturbative regime below the

¹ In [29] a quantum mechanical treatment of 4-derivative theories was suggested, which when suitably extended can tackle more complicated field theoretic systems. This can perhaps address issues of ghost and unitarity in a more robust manner.

Planck scale.

The ideas of induced gravity goes long back. It was first proposed in [36, 37], where the quantum matter fluctuations at high energy generate gravitational dynamics at low energy inducing cosmological and Newton’s gravitational constant. Another proposal suggested in [38–40] induces Einstein gravity spontaneously via symmetry breaking along the lines of Higgs mechanism. Later in [41–45] the idea of generation of Einstein gravity via dynamical symmetry breaking was considered, following the methodology of Coleman-Weinberg [46]. In [45], metric fluctuations were also incorporated in the generation of induced Newton’s constant. Around the same time induced gravity from weyl-theory was also studied [47–49]. Phase-transitions leading to generation of Einstein-Hilbert gravity due to loop-effects from conformal factor coupled with scalar field were studied in [50]. In [51, 52] the renormalization group improved effective-potential of the dilaton leads to running of VeV inducing masses (along with Einstein-Hilbert gravity). Furthermore the authors make a proposal along lines of [3, 4] to tackle ghost and tachyons. Cosmological consequences of these models were explored in [53, 54].

In this paper we therefore study scale-invariant gravitational and matter coupled systems in $(4 - \epsilon)$ dimensional regularisation scheme. The beta-functions are computed and compared with the past literature. The one-loop RG improved effective potential for the scalar field is computed by incorporating the quantum fluctuations of both matter and gravity [55]. The scale invariance is broken dynamically when the scalar-field ϕ acquires a VeV via Coleman-Weinberg mechanism [46]. This in turn induces gravitational Newton’s constant, cosmological constant and masses in the matter sector. We work in lorentzian signature and take the sign of $C_{\mu\nu\rho\sigma}^2$ (Weyl tensor square) to be negative, keeping the sign of R^2 term (where R is Ricci-scalar) to be always positive (this is done to avoid tachyonic instabilities). These choice of signs further allows necessary convergence in feynman $+i\epsilon$ -prescription by suppressing fields modes with large action in the lorentzian path-integral. The sign of the $R\phi^2$ term is taken negative, so to generate the right sign of Newton’s constant and to avoid tachyonic instabilities in the broken phase. The negative sign of $C_{\mu\nu\rho\sigma}^2$ term is taken in order to satisfy the unitary criterion as stated in [5, 6]. In this case we no longer have asymptotic freedom as has been observed in euclidean case in [9, 10, 16, 26, 30–33]. The VeV generated in RG improved effective potential has running, and therefore induces running in Newton’s constant and masses of matter fields. Due to the generation of Einstein-Hilbert term in the action, the propagator of metric fluctuations in the broken phase gets modified, and the modes acquires mass. In this broken phase we investigate the problem of spin-2 ghost by probing the running of its mass along the lines of [5, 6]².

The outline of paper is following. In section II the divergent part of the effective action is computed in $(4 - \epsilon)$ dimensional regularisation scheme. The beta-function are obtained from it. In section III one-loop renormalisation group improved effective potential for the scalar field is computed by incorporating quantum corrections from gravitational and matter degrees of freedom. In section IV the breaking of scale-invariance is studied via Coleman-

² These studies are conducted in the perturbative framework around the gaussian fixed point and is therefore different from studies done in the asymptotic safety scenario [56], where the RG running of couplings were computed using functional-renormalization group in euclidean signature [57–62], with spectral positivity [63] and ghost [64, 65] issues analysed around a non-gaussian fixed point. Present work is also different from the recent studies done in the direction of finite and ghost free non-local quantum field theories of gravity [66–69], in the sense as it doesn’t incorporates non-local features.

Weinberg mechanism, which in turn induces gravitational Newton's constant and masses in the broken phase. RG equation for VeV is derived, which induces a running in the generated Newton's constant and masses. In section V a prescription to avoid spin-2 massive ghost is given, where a procedure to pick the right set of initial conditions is stated. In section VI numerical analysis is done to give evidence showing that there exist a large domain of coupling parameter space where spin-2 massive ghost can be made physically unrealisable. Finally in section VII conclusions are presented.

II. RG RUNNING

In this section we compute the renormalisation group running of the various coupling parameters present in our scale-invariant theory. We start first with the formalism and compute the various diagrams that contain UV divergences. These are then used to write the beta-function of the various coupling parameters. We start by considering the path-integral of the coupled system ($\hbar = c = 1$)

$$Z = \int \mathcal{D}\gamma_{\mu\nu} \mathcal{D}\phi \mathcal{D}\bar{\psi} \mathcal{D}\psi \exp \left[i \left(S_{\text{GR}} + S_{\text{matter}} \right) \right], \quad (1)$$

where S_{GR} and S_{matter} are given by

$$\begin{aligned} S_{\text{GR}} &= \frac{1}{16\pi} \int d^d x \sqrt{-\gamma} \left[-\frac{1}{f^2} \left(R_{\mu\nu} R^{\mu\nu} - \frac{1}{3} R^2 \right) + \frac{\omega}{6f^2} R^2 \right], \\ S_{\text{matter}} &= \int d^d x \sqrt{-\gamma} \left[\frac{1}{2} \partial_\mu \phi \partial^\mu \phi - \frac{\lambda}{4} \phi^4 - \frac{\xi}{2} R \phi^2 + \bar{\psi} (i\gamma^\mu D_\mu - y_t \phi) \psi \right], \end{aligned} \quad (2)$$

where the coupling parameters f^2 , ω , λ , ξ and y_t are all dimensionless, and the geometric quantities (curvature and covariant-derivative) depends on metric $\gamma_{\mu\nu}$. In the fermionic part of action, the Dirac gamma matrices are defined via tetrads and inverse tetrads ($\gamma^\mu = e_a{}^\mu \gamma^a$, $\gamma_\mu = e^a{}_\mu \gamma_a$), and D_μ is the spin-connection covariant derivative.

$$D_\mu = \partial_\mu - \frac{i}{2} \sigma^{cd} \omega_{\mu cd}. \quad (3)$$

Here greek indices denote the space-time index, while the latin indices denote the internal lorentz index, and $\sigma_{cd} = i/4[\gamma_c, \gamma_d]$. The internal indices are raised and lowered using internal metric η_{ab} . For torsionless manifold the spin-connection can be expressed in terms of the christoffel connection $\Gamma_\mu{}^\alpha{}_\nu$ (which can be re-expressed again in terms of tetrads) as,

$$\omega_\mu{}^{ad} = \frac{1}{2} \left[e^{a\rho} (\partial_\mu e^d{}_\rho - \partial_\rho e^d{}_\mu) - e^{d\rho} (\partial_\mu e^a{}_\rho - \partial_\rho e^a{}_\mu) + e^b{}_\mu e^{a\rho} e^{d\nu} (\partial_\nu e_{b\rho} - \partial_\rho e_{b\nu}) \right]. \quad (4)$$

The dimensionless nature of coupling f^2 and ω/f^2 results in a fully dimensionless scale-invariant coupled action.

We study the diffeomorphism invariant action of the coupled system using background field method [70, 71] in $(4 - \epsilon)$ dimensional regularisation scheme. It is advantageous, as by construction it preserves background gauge invariance. The field is decomposed into background and fluctuation. Keeping the background fixed the path-integral is then reduced to

an integral over the fluctuations. The gravitational metric field is decomposed into background and fluctuation, while the tetrads (and its inverse) are expressed in powers of this fluctuation field. The matter fields are similarly decomposed. The gauge invariance of the full metric field is then transformed into the invariance over the fluctuation field. To prevent over-counting of gauge-orbits in the path-integral measure, a constraint is applied on this fluctuation field, which results in appearance of auxiliary fields called ghosts. The effective action generated after integrating over the fluctuation and auxiliary fields still enjoys invariance over the background fields.

The quantum metric is written as

$$\gamma_{\mu\nu} = \bar{g}_{\mu\nu} + h_{\mu\nu}, \quad (5)$$

where $\bar{g}_{\mu\nu}$ is some arbitrary (but fixed) background and $h_{\mu\nu}$ is the metric fluctuation. The full action can be expanded in powers of $h_{\mu\nu}$. The path-integral measure over $\gamma_{\mu\nu}$ is then replaced with measure over $h_{\mu\nu}$. Integrating over the fluctuation field implies that in some sense they will appear only as internal legs and never as external legs. The background gauge invariant effective action formalism allows to choose a particular background for the ease of computation. In particular writing $\bar{g}_{\mu\nu} = \eta_{\mu\nu} + H_{\mu\nu}$ (while still keeping $H_{\mu\nu}$ generic) allows one to use the machinery of the flat space-time QFT, thereby giving a particle interpretation to the internal ($h_{\mu\nu}$) and external ($H_{\mu\nu}$) legs, in the sense that the former behaves as virtual particle, while the later is the corresponding external particle. In this manner one can compute the effective action for the external leg $H_{\mu\nu}$. Alternatively one can expand the full action around flat space-time directly, calling the fluctuation to be $h'_{\mu\nu}$ though. This is a highly non-linear gauge theory with infinite number of interactions terms (however their couplings are related to each other by diffeomorphism invariance). Then following the usual strategy of background field method and writing $h'_{\mu\nu} = H_{\mu\nu} + h_{\mu\nu}$, it is quickly seen that $H_{\mu\nu}$ is the external leg corresponding to the virtual particle given by $h_{\mu\nu}$. Integrating over quantum fluctuations $h_{\mu\nu}$ then gives the effective action in terms of $H_{\mu\nu}$ field.

One can then set-up Feynman perturbation theory by expanding the original action in powers of $h_{\mu\nu}$ and $H_{\mu\nu}$. Similarly writing the scalar and fermion fields as

$$\phi = \varphi + \chi, \quad \bar{\psi} = \bar{\theta} + \bar{\eta}, \quad \psi = \theta + \eta, \quad (6)$$

one can expand the action in powers of fluctuations χ , η and $\bar{\eta}$. The piece which is quadratic in only fluctuations ($h_{\mu\nu}$, χ , η and $\bar{\eta}$) gives the propagator while all the other terms gives the interactions vertices. In one-loop approximation the terms which are exclusively quadratic in fluctuations are retained, all other terms which involve higher powers of fluctuations ($h_{\mu\nu}$, χ , η and $\bar{\eta}$) contribute in higher-loops and will be ignored here. In-fact for computing the running of all matter couplings (except ξ) it is sufficient to consider the situation with $H_{\mu\nu} = 0$. However, in the case for computing running of ξ , terms up-to (and at-least) linear in $H_{\mu\nu}$ should be retained. Similarly if one is interested in studying behaviour or R^2 and $R_{\mu\nu}R^{\mu\nu}$ then one should at-least retain terms up-to quadratic in $H_{\mu\nu}$.

A. Gauge Fixing and Ghosts

The path-integration over the gravitational field is ill defined. This is a general feature of gauge theories where the gauge invariance (diffeomorphism invariance for gravity) relates two field configuration by gauge transformation. Such field configuration will contribute

equally to the path-integral. However this will lead to over-counting. To prevent such over-counting, gauge-invariance needs to be broken by constraining the gauge field. This procedure of systematically applying the constraint leads to ghost, which are elegantly taken care of by the Faddeev-Popov prescription [72].

However in this style of breaking the invariance one may wonder whether the gauge (or diffeomorphism) invariance emerges in the effective action. To make sure that the effective action obtained after integrating out the fluctuation field is gauge invariant, background field method is followed. It is a method (and procedure) which guarantees that the effective action constructed using it will be background gauge invariant. Below we describe the procedure for gauge-fixing in the background field method.

The diffeomorphism invariance of the full action in eq (2) implies that for arbitrary vector field ϵ^ρ , the action should be invariant under the following transformation of the metric field variable,

$$\delta_D \gamma_{\mu\nu} = \mathcal{L}_\epsilon \gamma_{\mu\nu} = \epsilon^\rho \partial_\rho \gamma_{\mu\nu} + \gamma_{\mu\rho} \partial_\nu \epsilon^\rho + \gamma_{\nu\rho} \partial_\mu \epsilon^\rho, \quad (7)$$

where $\mathcal{L}_\epsilon \gamma_{\mu\nu}$ is the Lie derivative of the quantum metric $\gamma_{\mu\nu}$ along the vector field ϵ^ρ . Decomposing the quantum metric $\gamma_{\mu\nu}$ into background ($\bar{g}_{\mu\nu}$) and fluctuation ($h_{\mu\nu}$) allows one to figure out the transformation of the fluctuation field while keeping the background fixed. This will imply the following transformation of $h_{\mu\nu}$.

$$\delta_D h_{\mu\nu} = \bar{\nabla}_\mu \epsilon_\nu + \bar{\nabla}_\nu \epsilon_\mu + \epsilon^\rho \bar{\nabla}_\rho h_{\mu\nu} + h_{\mu\rho} \bar{\nabla}_\nu \epsilon^\rho + h_{\nu\rho} \bar{\nabla}_\mu \epsilon^\rho, \quad (8)$$

where $\bar{\nabla}$ is the covariant derivative whose connection is constructed using the background metric. This is the full transformation of the metric fluctuation field. Ignoring terms which are linear in $h_{\mu\nu}$ allows one to investigate only the one-loop effects. These ignored terms are however mandatory when dealing with higher-loop effects. The invariance of the action is broken by choosing an appropriate gauge-fixing condition implemented via Faddeev-Popov procedure.

The gauge fixing action chosen for fixing the invariance under the transformation of the metric fluctuation field is given by,

$$S_{GF} = \frac{1}{32\pi\alpha} \int d^d x \sqrt{-\bar{g}} \left(\bar{\nabla}^\rho h_{\rho\mu} - \frac{1+\rho}{d} \bar{\nabla}_\mu h \right) Y^{\mu\nu} \left(\bar{\nabla}^\sigma h_{\sigma\nu} - \frac{1+\rho}{d} \bar{\nabla}_\nu h \right), \quad (9)$$

where α and ρ are gauge parameters, while $Y_{\mu\nu}$ is either a constant or a differential operator depending upon the gravitational theory under consideration. For the theory considered here in eq. (2), we consider higher-derivative type gauge fixing with $Y_{\mu\nu} = (-\bar{g}_{\mu\nu} \bar{\square} + \beta \bar{\nabla}_\mu \bar{\nabla}_\nu)$, where $\bar{\square} = \bar{\nabla}_\mu \bar{\nabla}^\mu$. Choosing $\rho = -1$ and $\beta = 0$ correspond to Landau gauge condition. Taking $\alpha \rightarrow 0$ imposes the gauge condition sharply.

The ghost action is obtained following the Faddeev-Popov procedure [72]. In general if the gauge-fixing condition on the gravitational field $h_{\mu\nu}$ is written as $F_\mu = 0$ (which here is $F_\mu = \bar{\nabla}^\rho h_{\rho\mu} - \frac{1+\rho}{d} \bar{\nabla}_\mu h$), we introduce it in the path-integral by multiplying the later with unity in the following form,

$$1 = \int \mathcal{D}F_\mu^\epsilon (\det Y)^{\frac{1}{2}} \exp \left[\frac{i}{32\pi\alpha} \int d^d x \sqrt{-\bar{g}} F_\mu^\epsilon Y^{\mu\nu} F_\nu^\epsilon \right], \quad (10)$$

where F_μ^ϵ is the gauge transformed F_μ . As $Y^{\mu\nu}$ contains derivative operator, therefore its determinant is non-trivial. The original path-integral (without gauge-fixing) being invariant

under transformation eq. (8) of the field $h_{\mu\nu}$ implies that a change of integration variable from $h_{\mu\nu}$ to $h_{\mu\nu}^\epsilon$ doesn't give rise to any jacobian in the path-integral measure. However replacing the measure over F_μ^ϵ with measure over ϵ^ρ introduces a non-trivial jacobian in the path-integral. This is obtained as follows,

$$dF_\mu^\epsilon = \frac{\partial F_\mu^\epsilon}{\partial \epsilon^\rho} d\epsilon^\rho \quad \Rightarrow \quad \mathcal{D}F_\mu^\epsilon = \det\left(\frac{\partial F_\mu^\epsilon}{\partial \epsilon^\rho}\right) \mathcal{D}\epsilon^\rho. \quad (11)$$

In the background field formalism this jacobian consist of background covariant derivative, background and fluctuation fields, and is independent of the transformation parameter ϵ^ρ . This implies that it can be taken out of the functional integral over ϵ^ρ . Changing the integration variable from $h_{\mu\nu}^\epsilon$ to $h_{\mu\nu}$, and ignoring the infinite constant generated by integrating over ϵ^ρ , gives us the gauge fixed path integral including the determinant.

The functional determinant appearing in eq. (11) can be exponentiated by making use of appropriate auxiliary fields. Writing the functional determinant $(\det Y)^{1/2}$ as $(\det Y) \times (\det Y)^{-1/2}$, allows to combine the former with the Faddeev-Popov determinant in eq. (11), which is then exponentiated by making use of anti-commuting auxiliary fields, while the later $(\det Y)^{-1/2}$ is exponentiated by making use of commuting auxiliary fields. The former auxiliary fields are known as Faddeev-Popov ghosts, while those in later case are known as Nielsen-Kallosh ghosts [73, 74]. The path integral of the full ghost sector is given by,

$$\int \mathcal{D}\bar{C}_\mu \mathcal{D}C_\nu \mathcal{D}\theta_\alpha \exp\left[-i \int d^d x \sqrt{-\bar{g}} \left\{ \bar{C}_\mu \left(Y^{\mu\nu} \frac{\partial F_\nu}{\partial \epsilon^\rho} \right) C^\rho + \frac{1}{2} \theta_\alpha Y^{\alpha\beta} \theta_\beta \right\}\right], \quad (12)$$

where \bar{C}_μ and C_ν are Faddeev-Popov ghost fields arising from the gauge fixing in the gravitational sector, and θ_μ is the commuting ghost arising due to fact that $Y_{\mu\nu}$ contains derivatives.

In the case when F_μ is given as in eq. (9), the Faddeev-Popov ghost action is given by,

$$S_{\text{gh}}^{FP} = - \int d^d x \sqrt{-\bar{g}} \bar{C}_\mu X_\rho^\mu C^\rho, \quad (13)$$

where,

$$\begin{aligned} X_\rho^\mu = & (\bar{g}^{\mu\nu} \bar{\square} + \beta \bar{\nabla}^\mu \bar{\nabla}^\nu) \left[\bar{\nabla}_\rho \bar{\nabla}_\nu + \bar{g}_{\nu\rho} \bar{\square} - \frac{2(1+\rho)}{d} \bar{\nabla}_\nu \bar{\nabla}_\rho \right. \\ & + \bar{\nabla}_\rho h_{\sigma\nu} \bar{\nabla}^\sigma + \bar{\nabla}^\sigma \bar{\nabla}_\rho h_{\sigma\nu} + \bar{\nabla}^\sigma h_{\nu\rho} \bar{\nabla}_\sigma + h_{\nu\rho} \bar{\square} + \bar{\nabla}^\sigma h_{\sigma\rho} \bar{\nabla}_\nu + h_{\sigma\rho} \bar{\nabla}^\sigma \bar{\nabla}_\nu \\ & \left. - \frac{1+\rho}{d} \left(\bar{\nabla}_\rho h \bar{\nabla}_\nu + \bar{\nabla}_\nu \bar{\nabla}_\rho h + 2 \bar{\nabla}_\nu h_{\sigma\rho} \bar{\nabla}^\sigma + 2 h_{\sigma\rho} \bar{\nabla}_\nu \bar{\nabla}^\sigma \right) \right]. \quad (14) \end{aligned}$$

Here the last two lines contains terms linear in $h_{\mu\nu}$. These are not relevant in doing one-loop computations, but at higher-loops they are important. In the following we will ignore ghost contributions completely as they are not relevant in the computation of the running of matter couplings, while the running of gravitational couplings are taken from past literature [5, 6, 16, 26, 78].

B. Gravitational Field Propagator

The propagator for the gravitational field is obtained by expanding the gravitational action around the flat space-time up-to second order in the fluctuation field $h_{\mu\nu}$. By decomposing the fluctuation field in terms of various components and writing them using the

projection operators ($P_2^{\mu\nu\rho\sigma}$, $P_1^{\mu\nu\rho\sigma}$, $P_s^{\mu\nu\rho\sigma}$, $P_{sw}^{\mu\nu\rho\sigma}$, $P_{ws}^{\mu\nu\rho\sigma}$ and $P_w^{\mu\nu\rho\sigma}$) as given in appendix B, we note that this second variation can be expressed in a neat form in momentum space in the following manner,

$$\delta^2 S_{\text{GR}} = \frac{1}{32\pi} \int \frac{d^d q}{(2\pi)^d} h_{\mu\nu} \left[-\frac{q^4}{2f^2} P_2^{\mu\nu\rho\sigma} + \frac{q^4 \omega}{f^2} P_s^{\mu\nu\rho\sigma} \right] h_{\rho\sigma}. \quad (15)$$

Moreover the gauge-fixing action can be similarly expressed by using the projection operators,

$$S_{\text{GF}} = \frac{1}{32\pi\alpha} \int \frac{d^d q}{(2\pi)^d} h_{\mu\nu} q^4 \left[-\frac{1}{2} P_1^{\mu\nu\rho\sigma} + \frac{1-\beta}{d^2} \left\{ (1+\rho)^2 (d-1) P_s^{\mu\nu\rho\sigma} + (d-1-\rho)^2 P_w^{\mu\nu\rho\sigma} - \sqrt{d-1} (1+\rho)(d-1-\rho) (P_{sw}^{\mu\nu\rho\sigma} + P_{ws}^{\mu\nu\rho\sigma}) \right\} \right] h_{\rho\sigma}. \quad (16)$$

By writing the gauge-fixing action in terms of the projection operators allows us to see clearly which modes of the field are affected by the gauge-fixing. For example the spin-2 mode is not affected at all by the gauge-fixing condition. Interestingly it should be noted that there is another gauge-invariant mode of the field which arises due to the action of spin-2 projection operator on the $h_{\mu\nu}$ field (see appendix B). However under harmonic type gauge-fixing condition this mode doesn't remain completely unaffected. Only for some particular gauge choices this mode is not affected by the gauge-fixing condition. Landau gauge being one such choice $\rho = -1, \beta = 0, \alpha = 0$. In this gauge choice only the purely longitudinal modes are gauge fixed. In this gauge the propagator for the metric fluctuation field is the following,

$$D^{\mu\nu\rho\sigma} = (\Delta_G^{-1})^{\mu\nu\rho\sigma} = (16\pi) \frac{f^2}{q^4} \left(-2P_2^{\mu\nu\rho\sigma} + \frac{1}{\omega} P_s^{\mu\nu\rho\sigma} \right) = \sum_i Y_i(q^2) P_i^{\mu\nu\rho\sigma}, \quad (17)$$

where Y_i are the propagators for the various spin-components:

$$Y_2 = -(16\pi) \frac{2f^2}{q^4} \quad Y_s = (16\pi) \frac{f^2}{\omega q^4}. \quad (18)$$

Here $\Delta_G^{\mu\nu\alpha\beta}$ is the inverse propagator for the $h_{\mu\nu}$ field including the gauge fixing and is symmetric in $\mu\nu$ and $\alpha\beta$. As the propagator is $1/q^4$, it doesn't allow to be decomposed further via partial fractions. Here the first term in eq. (17) arises due the presence of $C_{\mu\nu\rho\sigma}^2$ part of action, while the later comes from the R^2 part. In this form it is not clear how the unitarity will be satisfied.

C. Formalism

We employ the background field formalism and decompose the metric and matter fields as in eq. (5 and 6) respectively, where we choose the background space-time to be flat. In order to do the one-loop computation the action is expanded up-to second powers of the all fluctuation field ($h_{\mu\nu}$, χ , η and $\bar{\eta}$). This will result in various vertices and propagators that

are required for the one-loop analysis. The second variation of the matter action is given by the following,

$$\begin{aligned}
\delta^2 S_{\text{matter}} = & \frac{1}{2} \int d^d x \left[\left(\frac{1}{4} h^2 - \frac{1}{2} h_{\mu\nu} h^{\mu\nu} \right) \left\{ \frac{1}{2} \partial_\alpha \varphi \partial^\alpha \varphi - \frac{\lambda}{4} \varphi^4 \right\} - \frac{1}{2} h h^{\mu\nu} \partial_\mu \varphi \partial_\nu \varphi \right. \\
& + h^{\mu\alpha} h_{\alpha\nu} \partial_\mu \varphi \partial_\nu \varphi - \frac{1}{2} \xi \varphi^2 \left(h \partial_\mu \partial_\nu h^{\mu\nu} - h \square h - 4 h^{\mu\nu} \partial_\mu \partial_\rho h^\rho{}_\nu + 2 h^{\mu\nu} \square h_{\mu\nu} + 2 h^{\mu\nu} \partial_\mu \partial_\nu h \right. \\
& \left. \left. - 2 \partial_\rho h^{\rho\sigma} \partial^\mu h_{\sigma\mu} + 2 \partial_\rho h^{\rho\sigma} \partial_\sigma h + \frac{3}{2} \partial_\mu h^{\rho\sigma} \partial^\mu h_{\rho\sigma} - \frac{1}{2} \partial_\mu h \partial^\mu h - \partial^\sigma h^{\rho\mu} \partial_\rho h_{\sigma\mu} \right) \right. \\
& \left. - \lambda \varphi^3 h \chi + h \partial_\mu \varphi \partial^\mu \chi - 2 h^{\mu\nu} \partial_\mu \varphi \partial_\nu \chi - 2 \xi \chi \varphi (\partial_\mu \partial_\nu h^{\mu\nu} - \square h) + \partial_\mu \chi \partial^\mu \chi - 3 \lambda \varphi^2 \chi^2 \right] \\
& + \int d^d x \left[\left\{ \left(\frac{1}{8} h^2 - \frac{1}{4} h_{\alpha\beta} h^{\alpha\beta} \right) \delta_\rho{}^\mu - \frac{1}{4} h h_\rho{}^\mu + \frac{3}{8} h_\rho{}^\alpha h_{\alpha\mu} \right\} \bar{\theta} i \gamma^\rho \partial_\mu \theta \right. \\
& + \frac{i}{4} \bar{\theta} \gamma^\rho [\gamma^\alpha, \gamma^\beta] \theta \left\{ -\frac{1}{4} h_\alpha{}^\sigma \partial_\rho h_{\beta\sigma} + \frac{1}{2} \partial_\alpha (h_{\beta\sigma} h^\sigma{}_\rho) + \frac{1}{2} h_\alpha{}^\sigma \partial_\sigma h_{\beta\rho} - \frac{1}{2} h \partial_\alpha h_{\beta\rho} \right\} \\
& - y_t \varphi \left(\frac{1}{8} h^2 - \frac{1}{4} h_{\alpha\beta} h^{\alpha\beta} \right) + \bar{\eta} \left\{ \frac{i}{2} \gamma^\rho (h \delta_\rho{}^\mu - h_\rho{}^\mu) \partial_\mu - \frac{i}{4} \gamma^\rho [\gamma^\alpha, \gamma^\beta] \partial_\alpha h_{\beta\rho} - \frac{1}{2} y_t \varphi h \right\} \theta \\
& + \bar{\theta} \left\{ \frac{i}{2} \gamma^\rho (h \delta_\rho{}^\mu - h_\rho{}^\mu) \partial_\mu - \frac{i}{4} \gamma^\rho [\gamma^\alpha, \gamma^\beta] \partial_\alpha h_{\beta\rho} - \frac{1}{2} y_t \varphi h \right\} \eta + \bar{\eta} (i \gamma^\rho \partial_\rho - y_t \varphi) \eta \\
& \left. - y_t \left(\chi \bar{\eta} \theta + \chi \bar{\theta} \eta + \frac{1}{2} h \chi \bar{\theta} \theta \right) \right]. \tag{19}
\end{aligned}$$

The various vertices and matter propagators are written in detail in appendix C. Having obtained the second variation giving propagator and the vertices, we set forth by considering the path-integral over the fluctuation fields. In this case the zeroth order term will be independent of the fluctuation fields and can be taken out of the path-integral. The linear term can be removed by doing field redefinition. In general, terms proportional to equation of motion can be removed by doing field redefinition. Such a redefinition will give rise to a trivial jacobian from the functional measure. The quadratic piece can now be investigated easily by putting together all the field fluctuations in the form of a multiplet $\Phi^T = (h_{\mu\nu}, \chi, \eta^T, \bar{\eta})$. Using this the path-integral can be written in a more compact form as,

$$Z[\mathbf{J}] = \exp \left[i \left(S_{\text{GR}}(\bar{g}) + S_{\text{matter}}(\varphi, \bar{\theta}, \theta) \right) \right] \int \mathcal{D}\Phi \exp \left[i \int d^d x \left(\frac{1}{2} \Phi^T \cdot \mathbf{M} \cdot \Phi + \Phi^T \cdot \mathbf{J} \right) \right], \tag{20}$$

where $\mathbf{J} = \{t_{\mu\nu}, t, \rho, \bar{\rho}^T\}$ is the source multiplet which couples with the fluctuation field multiplet $\Phi = (h_{\mu\nu}, \chi, \eta^T, \bar{\eta})$. The super matrix \mathbf{M} is given by

$$\mathbf{M} = \begin{bmatrix} \Delta_G^{\mu\nu\rho\sigma} + V^{\mu\nu\rho\sigma} + U^{\mu\nu\rho\sigma} & V_{h\phi}^{\mu\nu} & (V_{h\psi}^{\mu\nu})_b & (V_{h\bar{\psi}}^T)^{\mu\nu}_b \\ V_{\phi h}^{\rho\sigma} & \Delta_s - V_s & (V_{\phi\psi})_b & (V_{\phi\bar{\psi}}^T)_b \\ (V_{\psi h}^T)^{\rho\sigma}_a & (V_{\psi\phi}^T)_a & 0 & (\Delta_F^T)_{ab} + (V_{\bar{\psi}\psi}^T)_{ab} \\ (V_{\bar{\psi} h}^{\rho\sigma})_a & (V_{\bar{\psi}\phi})_a & (\Delta_F)_{ab} - (V_{\bar{\psi}\psi})_{ab} & 0 \end{bmatrix}. \tag{21}$$

From the generating functional Z , one can define the one-particle-irreducible (1PI) generating functional $\Gamma = W[\mathbf{J}] - \int d^d x \langle \Phi^T \rangle \cdot \mathbf{J}$, where $W[\mathbf{J}] = -i \ln Z[\mathbf{J}]$ and $\langle \Phi^T \rangle$ is the expectation

value of Φ^T field. The 1PI generating functional is also the effective action containing the quantum corrections. In the one-loop approximation (which we are considering here), one can perform the functional integral over the super-field Φ thereby giving an expression for the one-loop effective action to be,

$$\Gamma^{1\text{-loop}}[\Phi] = S_{\text{GR}}(\bar{g}) + S_{\text{matter}}(\varphi, \bar{\theta}, \theta) + \frac{i}{2} \text{STr} \ln \mathbf{M}, \quad (22)$$

where the first two terms correspond to tree-level diagrams while the last term contains one-loop quantum corrections. The appearance of generalised trace ‘STr’ means that

$$\text{STr} \begin{pmatrix} a & \alpha \\ \beta & b \end{pmatrix} = \text{Tr}(a) - \text{Tr}(b). \quad (23)$$

In the following we will be computing the divergent pieces present in the $\text{STr} \ln \mathbf{M}$. There are various ways to compute the one-loop quantum corrections. The most common methodology to do is via Feynman diagrams after computing vertices and propagator. Here we will follow a slightly different strategy of computation via evaluation of functional determinant. We start by writing $\mathbf{M} = \Delta + \mathbf{V}$, where the former Δ contains the various propagator while the later \mathbb{V} contains various vertices. They are given by,

$$\Delta = \begin{bmatrix} \Delta_G^{\mu\nu\rho\sigma} & 0 & 0 & 0 \\ 0 & \Delta_s & 0 & 0 \\ 0 & 0 & 0 & (\Delta_F^T)_{ab} \\ 0 & 0 & (\Delta_F)_{ab} & 0 \end{bmatrix}, \quad \mathbf{V} = \begin{bmatrix} V^{\mu\nu\rho\sigma} + U^{\mu\nu\rho\sigma} & V_{h\phi}^{\mu\nu} & (V_{h\psi}^{\mu\nu})_b & (V_{h\bar{\psi}}^T)^{\mu\nu} \\ V_{\phi h}^{\rho\sigma} & -V_s & (V_{\phi\psi})_b & (V_{\phi\bar{\psi}}^T)_b \\ (V_{\psi h}^T)^{\rho\sigma} & (V_{\psi\phi}^T)_a & 0 & (V_{\psi\bar{\psi}}^T)_{ab} \\ (V_{\bar{\psi}h}^{\rho\sigma})_a & (V_{\bar{\psi}\phi})_a & -(V_{\bar{\psi}\psi})_{ab} & 0 \end{bmatrix}. \quad (24)$$

Pulling out Δ from the expression for \mathbf{M} allows to expand the residual expression $(\mathbf{I} + \Delta^{-1} \cdot \mathbf{V})$ (where \mathbf{I} is a generalised identity in super-field space) under the logarithm in a perturbative manner as follows,

$$\text{STr} \ln \mathbf{M} = \text{STr} \ln \Delta \cdot (\mathbf{I} + \mathbb{V}) = \text{STr} \ln \Delta + \text{STr} \left[\mathbb{V} - \frac{1}{2} \mathbb{V}^2 + \frac{1}{3} \mathbb{V}^3 - \frac{1}{4} \mathbb{V}^4 + \dots \right]. \quad (25)$$

Here $\mathbb{V} = \Delta^{-1} \cdot \mathbf{V}$ is given by

$$\mathbb{V} = \begin{bmatrix} (\Delta_G^{-1})^{\mu\nu\rho\sigma} (V + U)_{\rho\sigma\alpha\beta} & (\Delta_G^{-1})^{\mu\nu\rho\sigma} (V_{h\phi})_{\rho\sigma} & (\Delta_G^{-1})^{\mu\nu\rho\sigma} (V_{h\psi})_{c\rho\sigma} & (\Delta_G^{-1})^{\mu\nu\rho\sigma} (V_{h\bar{\psi}}^T)_{c\rho\sigma} \\ \Delta_s^{-1} (V_{\phi h})_{\alpha\beta} & -\Delta_s^{-1} V_s & \Delta_s^{-1} (V_{\phi\psi})_c & \Delta_s^{-1} (V_{\phi\bar{\psi}}^T)_c \\ (\Delta_F^{-1})_{ab} (V_{\bar{\psi}h})_{b\alpha\beta} & (\Delta_F^{-1})_{ab} (V_{\bar{\psi}\phi})_b & -(\Delta_F^{-1})_{ab} (V_{\bar{\psi}\psi})_{bc} & 0 \\ (\Delta_F^{-1})_{ab}^T (V_{\psi h}^T)_{b\alpha\beta} & (\Delta_F^{-1})_{ab}^T (V_{\psi\phi}^T)_b & 0 & (\Delta_F^{-1})_{ab}^T (V_{\psi\bar{\psi}}^T)_{bc} \end{bmatrix}. \quad (26)$$

It should be mentioned here that so far we took background metric to be flat with $H_{\mu\nu} = 0$. This is enough to compute the counter-terms involving quantum gravity corrections to all matter couplings including their anomalous dimensions. If we had included terms with $H_{\mu\nu} \neq 0$, then it is also possible to compute the counter-term proportional to $R\varphi^2$. But here for simplicity we keep $H_{\mu\nu} = 0$, and the counter-term proportional to $R\varphi^2$ will be computed using methodology of heat-kernels (HK) later. Heat-kernel method is quick, as the HK coefficients have already been computed in past [75–78]. Besides, it also gives an alternative check on the computation done using feynman diagrams. For flat background the term $\text{STr} \ln \Delta$ is irrelevant, but it is not so if the background is non-flat for which case

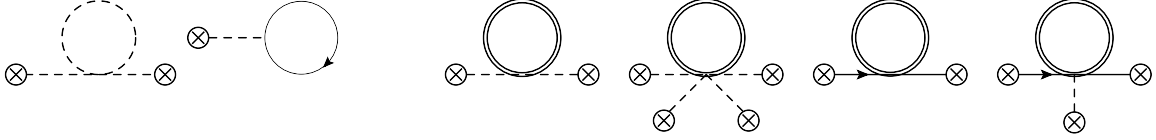


FIG. 1: Various diagrams containing divergences at the tadpole level. Here the dashed line represent scalar field, solid line with arrow represent fermion field while double-line represent $h_{\mu\nu}$ -field. The first two graphs are purely matter ones, while the other four graphs contain quantum gravity corrections.

this gives purely curvature dependent divergent contributions. Such contributions have been computed elsewhere in literature [16, 78] and here we will just take their results.

In the following we will be computing the various graphs that are giving quantum gravity corrections to the running of the matter couplings and the fields anomalous dimensions.

D. Graphs

Here we will be computing the various graphs that contain divergent contributions. These are basically the terms in the series expansion given in eq. (25), which will be evaluated one by one. The first term of the series contain tadpole graphs (those having single vertex), the second term of series has bubble graphs (those having two vertices), the third term of the series are triangle graphs containing three vertices while the fourth term of series are square graphs with four vertices. The series has infinite number of graphs, but the divergent ones are only present in the first four terms of the series expansion, and below we will be computing them.

1. Tadpole

These set of graphs arises from the first term of the series in eq. (25) which is $S\text{Tr}(\mathbb{V}) = S\text{Tr}(\Delta^{-1} \cdot \mathbf{V})$. Here the super-trace takes care of trace over bosonic and fermionic part, and includes the trace not only over field space but also over lorentz indices. This will imply the following,

$$\begin{aligned} S\text{Tr}\mathbb{V} &= \text{Tr} [\mathbb{V}_{11} + \mathbb{V}_{22} - \mathbb{V}_{33} - \mathbb{V}_{44}] \\ &= \text{Tr} \left[(\Delta_G^{-1})^{\mu\nu\rho\sigma} (V + U)_{\rho\sigma\alpha\beta} - \Delta_s^{-1} V_s + (\Delta_F^{-1})_{ab} (V_{\bar{\psi}\psi})_{bc} - (\Delta_F^{-1})_{ab}^T (V_{\bar{\psi}\psi}^T)_{bc} \right]. \end{aligned} \quad (27)$$

Here the first term contains graphs having an internal graviton line, while the next three terms contains the usual diagrams which are present without gravity. The former gives quantum gravity contribution. The set of graphs present in the tadpole order are shown in figure 1.

Each of these diagrams can be evaluated using the vertices given in appendix C 2. Here we will write their contribution. However, the last three terms in eq. (27) vanish in scale-invariant theory. The gravitational ones are complicated and lengthy as the vertices are

cumbersome. Below we write this

$$\begin{aligned} \text{Tr} \{ (\Delta_G^{-1})^{\mu\nu\rho\sigma} V_{\rho\sigma\alpha\beta} \} &= \frac{1}{4} \int d^d x \left[\frac{d-4}{2d} (\partial\varphi)^2 - \frac{\lambda}{4} \varphi^4 \right] \int \frac{d^d p}{(2\pi)^d} \{ -(d-2)(d+1)Y_2 \\ &+ (d-3)Y_s \} + \frac{(d-2)\xi}{8} \int d^d x \varphi^2 \int \frac{d^d p}{(2\pi)^d} p^2 \{ (d+1)Y_2 - 2Y_s \}. \end{aligned} \quad (28)$$

For the other one there is more algebra as it involves Dirac-matrices. Here we will write the expression after performing the lorentz and Dirac matrix algebra. This is given by,

$$\begin{aligned} \text{Tr} \{ (\Delta_G^{-1})^{\mu\nu\rho\sigma} U_{\rho\sigma\alpha\beta} \} &= \frac{(d-2)(d+1)}{4} \int d^d x \left[\frac{3-2d}{2d} \bar{\theta} i \gamma^\alpha \partial_\alpha \theta + y_t \varphi \bar{\theta} \theta \right] \int \frac{d^d p}{(2\pi)^d} Y_2 \\ &+ \int d^d x \left[\frac{d^2-5d+5}{4d} \bar{\theta} i \gamma^\alpha \partial_\alpha \theta - \frac{d-3}{4} y_t \varphi \bar{\theta} \theta \right] \int \frac{d^d p}{(2\pi)^d} Y_s. \end{aligned} \quad (29)$$

The momentum integrals can be evaluated in the $(4-\epsilon)$ dimensional regularisation scheme and the divergent piece can be singled out easily. The divergent piece of all the above tadpole contribution is,

$$\begin{aligned} \Gamma_{\text{div}}^{\text{Tad}} &= -\frac{\mu^\epsilon}{16\pi^2\epsilon} \frac{M^2}{Z} \left[\frac{\lambda}{8} \left(10 + \frac{1}{2\omega} \right) \int d^d x \varphi^4 - \left(\frac{25}{8} + \frac{1}{16\omega} \right) \int d^d x \bar{\theta} (i\gamma^\mu \partial_\mu) \theta \right. \\ &\quad \left. + 5y_t \left(1 + \frac{1}{4\omega} \right) \int d^d x \bar{\theta} \varphi \theta \right], \end{aligned} \quad (30)$$

where $M^2/Z = 16\pi f^2$ is introduced for convenience.

2. Bubble

These set of graphs arise from second term in eq. (25) which is $-1/2\text{STr}(\Delta^{-1} \cdot \mathbf{V})^2$. Here again the super trace is evaluated as before. This will imply,

$$\text{STr} \mathbb{V}^2 = \text{Tr} [(\mathbb{V}^2)_{11} + (\mathbb{V}^2)_{22} - (\mathbb{V}^2)_{33} - (\mathbb{V}^2)_{44}]. \quad (31)$$

Here each of the term will contain several diagrams, but only few contain the divergences that are relevant for our purpose. These diagrams contain two vertices. They can be classified in three categories: (a) those with two internal graviton lines, (b) those with one internal graviton and one internal matter line and (c) those with two internal matter lines. The set of diagrams are shown in figure 2.

Each of these diagrams can be evaluated using the vertices given in appendix C 2. The super-trace given in eq. (31) contains lot of diagrams, but not all contain UV divergence. Here we will mention only the ones having the UV divergences. These come from,

$$\begin{aligned} &\text{Tr} \left[\Delta_s^{-1} V_s \Delta_s^{-1} V_s + 2\Delta_s^{-1} (V_{\phi\psi})_c (\Delta_F^{-1})_{cd} (V_{\bar{\psi}\phi})_d + 2\Delta_s^{-1} (V_{\phi\psi}^T)_c (\Delta_F^{-1})_{cd}^T (V_{\bar{\psi}\phi}^T)_d \right. \\ &- (D_F^{-1})_{ab} (V_{\bar{\psi}\psi})_{bd} (\Delta_F^{-1})_{de} (V_{\bar{\psi}\psi})_{ec} - (D_F^{-1})_{ab}^T (V_{\bar{\psi}\psi}^T)_{bd} (\Delta_F^{-1})_{de}^T (V_{\bar{\psi}\psi}^T)_{ec} \\ &+ (\Delta_G^{-1})^{\mu\nu\rho\sigma} V_{\rho\sigma\alpha\beta} (\Delta_G^{-1})^{\alpha\beta\theta\tau} V_{\theta\tau\mu'\nu'} + 2 (\Delta_G^{-1})^{\mu\nu\rho\sigma} (V_{h\phi})_{\rho\sigma} \Delta_s^{-1} (V_{\phi h})_{\mu'\nu'} \\ &+ 2 (\Delta_G^{-1})^{\mu\nu\rho\sigma} (V_{h\psi})_{\rho\sigma c} (\Delta_F^{-1})_{cd} (V_{\bar{\psi}h})_{d\mu'\nu'} \\ &\left. + 2 (\Delta_G^{-1})^{\mu\nu\rho\sigma} (V_{h\bar{\psi}}^T)_{c\rho\sigma} (\Delta_F^{-1})_{cd}^T (V_{\bar{\psi}h}^T)_{d\mu'\nu'} \right]. \end{aligned} \quad (32)$$

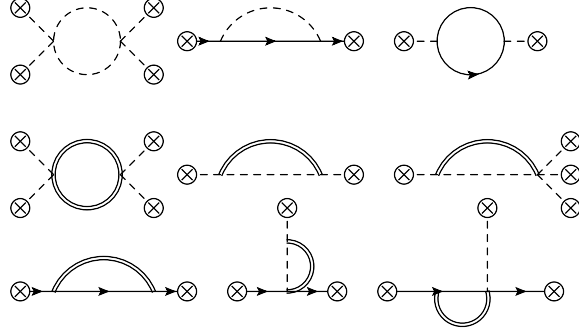


FIG. 2: Various diagrams containing divergences with two vertices. Here the dashed line represent scalar field, solid line with arrow represent fermion field while double-line represent $h_{\mu\nu}$ -field. Here the graphs on the first line are purely matter ones. The second and third line contain graphs having quantum gravity corrections.

From the various terms written in eq. (32) the first two lines contain diagrams which are purely matter ones and correspond to the diagrams shown in first row of figure 2, while the last two lines contain diagrams having quantum contributions and correspond to the diagrams shown in last two rows of the figure 2. The trace is over the Lorentz and space-time indices. After performing the algebra over Dirac matrices and doing the contraction of the tensors we get the simplified expression involving momentum integrals. The divergent contributions of the purely matter diagrams is,

$$\frac{i}{16\pi^2} \frac{1}{\epsilon} \left[9\lambda^2 \int d^4x \varphi^4 + 2y_t^2 \int d^4x \left\{ \bar{\theta} i \not{\partial} \theta + 2\partial_\mu \varphi \partial^\mu \varphi \right\} \right]. \quad (33)$$

The diagrams containing the internal graviton legs are bit complicated, as it involves lengthy Dirac matrix algebra and tensor manipulations. For doing these we have used various tricks to extract the divergent piece and also used MATHEMATICA packages (xAct [79], xTras [80] and FEYNALC [81]). Below for simplicity we will mention only the divergent piece of these diagrams to evade unnecessary complications, while some of the details will be mentioned in the appendix. The diagrams with internal graviton line has the following contributions

$$\begin{aligned} & \frac{i}{16\pi^2} \frac{1}{\epsilon} \left[\left\{ \frac{\xi^2}{4} \left(\frac{M^2}{Z} \right)^2 \left(5 + \frac{1}{\omega^2} \right) + \frac{6\xi\lambda M^2}{Z\omega} \right\} \int d^4x \varphi^4 + \frac{3M^2}{8Z\omega} \int d^4x \partial_\mu \varphi \partial^\mu \varphi \right. \\ & \left. + \frac{M^2}{Z\omega} \left\{ \frac{9}{4} \int d^4x \bar{\theta} i \not{\partial} \theta + 3(2\xi - 1)y_t \int d^4x \varphi \bar{\theta} \theta \right\} \right]. \quad (34) \end{aligned}$$

Here the first row contains contributions to the scalar sector, while the second row contain contributions to the fermion sector. The former correspond to diagrams of the second row in figure 2, while the later correspond to diagrams in the third row of figure 2 respectively.

Putting together the full contribution of the bubble kind of diagrams, we get contribution to the one-loop effective action of the diagrams having two vertices. This is given by,

$$\Gamma_{\text{div}}^{\text{Bub}} = -\frac{1}{16\pi^2} \frac{1}{\epsilon} \left[\left\{ 2y_t^2 + \frac{3M^2}{16Z\omega} \right\} \int d^4x \partial_\mu \varphi \partial^\mu \varphi + \left\{ \frac{9\lambda^2}{2} + \frac{3\xi\lambda M^2}{Z\omega} \right\} \int d^4x \varphi^4 \right]$$

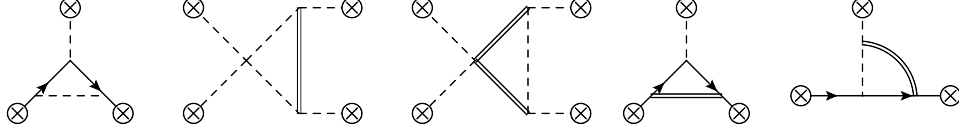


FIG. 3: Various diagrams containing divergences with three vertices. Here the first graph is purely matter oriented and gives correction to yukawa coupling. The next two diagrams are giving correction to φ^4 coupling. They are only present in the quantum gravity context. The last two diagrams are giving quantum gravity correction to the yukawa coupling.

$$\begin{aligned}
& + \frac{1}{2} \left(\frac{\xi M^2}{2Z} \right)^2 \left(5 + \frac{1}{\omega^2} \right) \int d^4x \varphi^4 + \left(y_t^2 + \frac{9M^2}{8Z\omega} \right) \int d^4x \bar{\theta} i \not{\partial} \theta \\
& + \frac{3(2\xi - 1)y_t M^2}{2 Z\omega} \int d^4x \varphi \bar{\theta} \theta \Big]. \tag{35}
\end{aligned}$$

3. Triangular Graphs

These diagram are generated from the third order terms in the series of eq. (25), $1/3\text{STr}\mathbb{V}^3$ where

$$\text{STr}\mathbb{V}^3 = \text{Tr} [(\mathbb{V}^3)_{11} + (\mathbb{V}^3)_{22} - (\mathbb{V}^3)_{33} - (\mathbb{V}^3)_{44}]. \tag{36}$$

These diagrams have three vertices and consist of graphs which are either purely matter oriented or ones which include a mixture of matter and gravity. These graphs give correction to vertex: either to φ^4 or to yukawa vertex $\varphi\bar{\theta}\theta$. On expansion we will see that there are many diagrams but we will consider those which carry divergent pieces and give correction to running couplings. Here we will only mention the trace pieces which will be carrying the divergences, however in principle there will be many more diagrams. The relevant terms in the trace which will be of relevance can be guessed by looking at the set of third order diagrams in figure 3. These are given by,

$$\begin{aligned}
& 3\text{Tr} \left[\Delta_s^{-1} (V_{\phi\bar{\psi}}^T)_a (\Delta_F^{-1})_{ab}^T (V_{\bar{\psi}\psi}^T)_{bc} (\Delta_F^{-1})_{cd}^T (V_{\psi\phi}^T)_d - \Delta_s^{-1} (V_{\phi\psi})_a (D_F^{-1})_{ab} (V_{\bar{\psi}\psi})_{bc} (\Delta_F^{-1})_{cd} (V_{\bar{\psi}\phi})_d \right. \\
& + (\Delta_G^{-1})^{\mu\nu\rho\sigma} \left\{ (V_{h\phi})_{\rho\sigma} \Delta_s^{-1} (V_{\phi h})^{\alpha\beta} (\Delta_G^{-1})_{\alpha\beta\theta\tau} V^{\theta\tau\gamma\delta} - (V_{h\phi})_{\rho\sigma} \Delta_s^{-1} V_s \Delta_s^{-1} (V_{\phi h})^{\alpha\beta} \right. \\
& + (V_{h\phi})_{\rho\sigma} \Delta_s^{-1} (V_{\phi\psi})_a (\Delta_F^{-1})_{ab} (V_{\bar{\psi}h})_{b\alpha\beta} + (V_{h\phi})_{\rho\sigma} \Delta_s^{-1} (V_{\phi\bar{\psi}}^T)_a (\Delta_F^{-1})_{ab}^T (V_{\psi h})_{b\mu\nu} \\
& + (V_{h\psi})_{a\rho\sigma} (\Delta_F^{-1})_{ab} (V_{\bar{\psi}\phi})_b \Delta_s^{-1} (V_{\phi h})_{\alpha\beta} + (V_{h\bar{\psi}}^T)_{a\rho\sigma} (D_F^{-1})_{ab}^T (V_{\psi\phi}^T)_b \Delta_s^{-1} (V_{\phi h})_{\alpha\beta} \\
& - (V_{h\psi})_{a\rho\sigma} (\Delta_F^{-1})_{ab} (V_{\bar{\psi}\psi})_{bc} (\Delta_F^{-1})_{cd} (V_{h\psi})_{d\alpha\beta} \\
& \left. + (V_{h\bar{\psi}}^T)_{a\rho\sigma} (\Delta_F^{-1})_{ab}^T (V_{\bar{\psi}\psi}^T)_{bc} (\Delta_F^{-1})_{cd}^T (V_{\psi h}^T)_{d\alpha\beta} \right\}. \tag{37}
\end{aligned}$$

Here the first line correspond to set of diagrams of purely matter type, while the rest of terms contain quantum gravity corrections. The second line contribute to running of φ^4 coupling while the rest of the terms correspond to the running of yukawa coupling. Interestingly while doing the computation involving fermions it is noticed that not all of terms are non-zero. The divergent contributions of these diagrams and corresponding their contribution to the effective action is given by,

$$\Gamma_{\text{div}}^{\text{Triangle}} = -\frac{1}{16\pi^2} \frac{1}{\epsilon} \int d^4x \left[\left(2y_t^3 - \frac{3M^2\xi}{Z\omega} y_t \right) \varphi \bar{\theta} \theta + \left(\frac{9M^2}{Z\omega} \lambda \xi^2 + \frac{3M^4}{2Z^2\omega^2} \xi^3 \right) \varphi^4 \right]. \tag{38}$$



FIG. 4: Various diagrams containing divergences with four vertices. Here there are only two diagrams. The first one is purely matter while the second one contain quantum gravity correction. Both give correction to the φ^4 coupling.

4. Square Graphs

These set of contribution arise at fourth order of the perturbative expansion given in the series eq. (25) and comes from $-1/4\text{STr}\mathbb{V}^4$. Here again the super-trace is given by,

$$\text{STr}\mathbb{V}^4 = \text{Tr} [(\mathbb{V}^4)_{11} + (\mathbb{V}^4)_{22} - (\mathbb{V}^4)_{33} - (\mathbb{V}^4)_{44}] . \quad (39)$$

These diagrams consist of four vertices and all of them contribute to the running of φ^4 coupling. There are only two diagrams at this order. One is purely matter type, contains a fermion loop with four external scalar legs, while the other one contains quantum gravity correction. The trace can be expanded as before and consists of large number of graphs but the ones containing the divergences are only two. These are the following,

$$2\text{Tr} \left[-(\Delta_F^{-1})_{ab}(V_{\bar{\psi}\psi})_{bc}(\Delta_F^{-1})_{cd}(V_{\bar{\psi}\psi})_{de}(\Delta_F^{-1})_{ef}(V_{\bar{\psi}\psi})_{fg}(\Delta_F^{-1})_{gk}(V_{\bar{\psi}\psi})_{kl} \right. \\ \left. + (\Delta_G^{-1})^{\mu\nu\rho\sigma}(V_{h\phi})_{\rho\sigma}\Delta_s^{-1}(V_{\phi h})^{\alpha\beta}(\Delta_G^{-1})_{\alpha\beta\theta\tau}(V_{h\phi})^{\theta\tau}\Delta_s^{-1}(V_{\phi h})_{\gamma\delta} \right] . \quad (40)$$

Here the former term is purely matter and contains a fermion loop, while the second term contain virtual gravitons. Considering as before just the divergent part and their corresponding contribution to the effective action, we find that,

$$\Gamma_{\text{div}}^{\text{Square}} = -\frac{1}{\epsilon} \frac{1}{16\pi^2} \left(-2y_t^4 + \frac{9M^4}{2Z^2\omega^2}\xi^4 \right) \int d^4x \varphi^4 . \quad (41)$$

5. $R\varphi^2$ divergence

Here we compute the divergence proportional to $R\varphi^2$. There are two ways to compute it. The first is via computation of feynman graphs and second via heat kernel. Conceptually both are same and give same results, however the later is quicker. In each case we break the metric $\gamma_{\mu\nu}$ appearing in path-integral is written as in eq. (5). In the former the background is further written as $\eta_{\mu\nu} + H_{\mu\nu}$ (see also paragraph following eq. (5)). Here $H_{\mu\nu}$ will act as external graviton for the corresponding internal leg $h_{\mu\nu}$. The action is then expanded under this decomposition. This way we get additional vertices. The vertices in the previous section are the ones for which $H_{\mu\nu} = 0$. If $H_{\mu\nu} \neq 0$ then we get contributions which contains dependence on external graviton leg, and if there are derivatives acting on $H_{\mu\nu}$, then those will give terms proportional to background curvature. This was employed in [26].

Alternatively, one can take the background metric $\bar{g}_{\mu\nu}$ to be maximally symmetric and compute the contributions proportional to background curvature using Heat-Kernel. This

will project directly the contribution proportional to $\bar{R}\varphi^2$. We use the heat-kernel methodology to compute the one-loop divergence proportional to $\bar{R}\varphi^2$. The matter fields are decomposed as in eq. (6), but this time we take background matter fields to be constant. The fluctuation metric $h_{\mu\nu}$ is further decomposed into various components as

$$h_{\mu\nu} = h_{\mu\nu}^{TT} + \bar{\nabla}_\mu \xi_\nu + \bar{\nabla}_\nu \xi_\mu + \bar{\nabla}_\mu \bar{\nabla}_\nu \sigma - \frac{1}{4} \bar{g}_{\mu\nu} \bar{\square} \sigma + \frac{1}{4} \bar{g}_{\mu\nu} h, \quad (42)$$

where

$$h_\mu^{TT\mu} = 0, \quad \bar{\nabla}^\mu h_{\mu\nu}^{TT} = 0, \quad \bar{\nabla}^\mu \xi_\mu = 0. \quad (43)$$

This decomposition of $h_{\mu\nu}$ introduces jacobians in the path-integral, which can be cancelled by redefining the fields as

$$\hat{\xi}_\mu = \sqrt{-\bar{\square} - \frac{\bar{R}}{4}} \xi_\mu, \quad \hat{\sigma} = \sqrt{-\bar{\square} \left(-\bar{\square} - \frac{\bar{R}}{3} \right)} \sigma. \quad (44)$$

Under this decomposition the Hessian for the fluctuation fields is obtained on a maximally symmetric background. This will be same as in eq. (20), except now \mathbf{M} will be different. The multiplet Φ also gets modified $\Phi^T = \left(h_{\mu\nu}^{TT}, \hat{\xi}_\mu, \hat{\sigma}, h, \chi, \eta^T, \bar{\eta} \right)$. As the background matter fields are constant, therefore the fermion sector is completely decoupled with mixing of fermion fluctuation field with metric and scalar fluctuations. This is not so when background matter is not constant. On the maximally symmetric background metric with constant background matter the matrix \mathbf{M} is given by (in the Landau gauge $\rho = -1$)

$$\begin{aligned} \int d^d x \sqrt{-\bar{g}} \Phi^T \mathbf{M} \Phi &= \int d^d x \sqrt{-\bar{g}} \left[h_{\mu\nu}^{TT} \Delta_2 (h^{TT})^{\mu\nu} + \hat{\xi}_\mu \Delta_1 \hat{\xi}^\mu \right. \\ &\left. + \begin{pmatrix} \hat{\sigma} & h & \chi \end{pmatrix} \begin{pmatrix} S_{\hat{\sigma}\hat{\sigma}} & S_{\hat{\sigma}h} & S_{\hat{\sigma}\phi} \\ S_{h\hat{\sigma}} & S_{hh} & S_{h\phi} \\ S_{\phi\hat{\sigma}} & S_{\phi h} & S_{\phi\phi} \end{pmatrix} \begin{pmatrix} \hat{\sigma} \\ h \\ \chi \end{pmatrix} + \frac{1}{2} \bar{\eta} \Delta_{1/2} \eta - \frac{1}{2} \eta^T \Delta_{1/2}^T \bar{\eta}^T \right], \end{aligned} \quad (45)$$

where

$$\begin{aligned} \Delta_2 &= \left\{ -\frac{Z}{M^2} \bar{\square}^2 + \left(-\xi \varphi^2 + \frac{(3+2\omega)Z\bar{R}}{3M^2} \right) \frac{\bar{\square}}{4} + \left(\frac{\lambda \varphi^4}{8} + \frac{\xi \bar{R} \varphi^2}{6} + \frac{(1+\omega)Z\bar{R}^2}{36M^2} \right) \right\}, \\ \Delta_1 &= \left\{ \frac{\bar{\square}^2}{\alpha} + \frac{\bar{R}\bar{\square}}{4\alpha} + \frac{\lambda \varphi^4 + \xi \bar{R} \varphi^2}{4} \right\}, \\ S_{\hat{\sigma}\hat{\sigma}} &= \left[\left(\frac{3}{\alpha} + \frac{Z\omega}{M^2} \right) \frac{3\bar{\square}^2}{16} + \left(\frac{6\alpha\xi\varphi^2 + 21\bar{R}}{64\alpha} \right) \bar{\square} + \frac{3\lambda\varphi^4}{32} + \frac{3\xi\bar{R}\varphi^2}{32} + \frac{3\bar{R}^2}{64\alpha} \right], \\ S_{h\hat{\sigma}} &= S_{\hat{\sigma}h} = \sqrt{-\bar{\square} \left(-\bar{\square} - \frac{\bar{R}}{3} \right)} \left[\left(\frac{1}{\alpha} - \frac{Z\omega}{M^2} \right) \frac{3\bar{\square}}{16} + \frac{3\bar{R} - 6\alpha\xi\varphi^2}{64\alpha} \right], \\ S_{\hat{\sigma}\phi} &= S_{\phi\hat{\sigma}} = -\frac{3\xi\varphi}{4} \sqrt{-\bar{\square} \left(-\bar{\square} - \frac{\bar{R}}{3} \right)}, \quad S_{h\phi} = S_{\phi h} = \frac{(3\xi\bar{\square} - \xi\bar{R} - 2\lambda\varphi^2)\varphi}{4}, \\ S_{hh} &= \left[\left(\frac{1}{\alpha} + \frac{3Z\omega}{M^2} \right) \frac{\bar{\square}^2}{16} + \left\{ \left(\frac{1}{\alpha} + \frac{4Z\omega}{M^2} \right) \frac{\bar{R}}{64} + \frac{3}{32} \xi \varphi^2 \right\} \bar{\square} - \frac{\lambda \varphi^4}{32} \right], \\ S_{\phi\phi} &= -\bar{\square} - \xi \bar{R} - 3\lambda \varphi^2, \\ \Delta_{1/2} &= (i\gamma^\mu \bar{\nabla}_\mu - m - y_t \varphi), \quad \Delta_{1/2}^T = (-i\gamma^{T\mu} \bar{\nabla}_\mu - m - y_t \varphi). \end{aligned} \quad (46)$$

We will not be considering the contribution for the ghost here, as they will not contribute at one-loop to the term proportional to $\bar{R}\varphi^2$. The one-loop effective action is given by,

$$\begin{aligned} \Gamma^{(1)} = & \frac{(d+1)(d-2)i}{4} \text{Tr} \ln \Delta_2 + \frac{(d-1)i}{2} \text{Tr} \ln \Delta_1 \\ & + \frac{i}{2} \text{Tr} \ln \left[\det \begin{pmatrix} S_{\hat{\sigma}\hat{\sigma}} & S_{\hat{\sigma}h} & S_{\hat{\sigma}\phi} \\ S_{h\hat{\sigma}} & S_{hh} & S_{h\phi} \\ S_{\phi\hat{\sigma}} & S_{\phi h} & S_{\phi\phi} \end{pmatrix} \right] - i \text{Tr} \ln \Delta_{1/2}. \end{aligned} \quad (47)$$

These functional traces can be tackled using heat-kernel [75–78]. One can compute the divergent part of the effective action from this. Since the background matter fields are not constant therefore this will however not be able to give the anomalous dimensions of the matter fields. However, the anomalous dimension has already been computed earlier using feynman diagram therefore it will not be considered again here. Here we will just look the divergent contribution proportional to $\bar{R}\varphi^2$, which is given by,

$$\Gamma_{\text{div}}^{R\varphi^2} = -\frac{1}{16\pi^2\epsilon} \left[\frac{\lambda}{2}(1+6\xi) + \frac{1}{3}y_t^2 + \frac{M^2}{Z\omega} \frac{\xi}{48}(7+120\xi+144\xi^2) - \frac{5M^2}{6Z}\xi\omega \right] \int d^4x \sqrt{-\bar{g}} \bar{R}\varphi^2. \quad (48)$$

Here the first two terms arise due to matter loop while the rest of terms contain quantum gravity corrections. This is in agreement with [26].

E. Effective action and Beta Functions

Once we have computed all the relevant graphs at various order of the perturbation theory and their divergent contributions, it is easy to put them together to write the divergent part of effective action and collect all the pieces together. The divergent part of the full effective action is given by,

$$\begin{aligned} \Gamma_{\text{div}}^{(1)} = & -\frac{1}{16\pi^2\epsilon} \int d^4x \left[\left(\frac{3M^2}{16Z\omega} + 2y_t^2 \right) (\partial\varphi)^2 + \left\{ \frac{9\lambda^2}{2} - 2y_t^4 + \frac{5M^2}{8Z} \left(2\lambda + \frac{M^2}{Z}\xi^2 \right) \right. \right. \\ & + \frac{M^2}{Z\omega} \frac{\lambda}{16} (1 + 48\xi + 144\xi^2) + \frac{M^4}{8Z^2\omega^2} \xi^2 (1 + 6\xi)^2 \left. \right\} \varphi^4 + \left\{ \frac{\lambda}{2} (1 + 6\xi) + \frac{1}{3}y_t^2 \right. \\ & + \frac{M^2}{Z\omega} \frac{\xi}{48} (7 + 120\xi + 144\xi^2) - \frac{5M^2}{6Z} \xi\omega \left. \right\} R\varphi^2 + \left\{ y_t^2 - \frac{25M^2}{8Z} + \frac{17M^2}{16Z\omega} \right\} \bar{\theta}i\cancel{\theta}\theta \\ & + \left. \left\{ 2y_t^3 + \frac{5M^2}{Z}y_t - \frac{5M^2}{4Z\omega}y_t \right\} \varphi\bar{\theta}\theta \right]. \end{aligned} \quad (49)$$

Once the divergent part of the effective action is written it is easy to compute the beta-function of the various couplings by incorporating the effect of the wave-function renormal-

isation. These are given by,

$$\eta_\varphi = \frac{d \ln Z_\varphi}{dt} = \frac{1}{16\pi^2} \left[\frac{3M^2}{8Z\omega} + 4y_t^2 \right], \quad (50)$$

$$\eta_\psi = \frac{d \ln Z_\psi}{dt} = \frac{1}{16\pi^2} \left[y_t^2 - \frac{25M^2}{8Z} + \frac{17M^2}{Z\omega} \right], \quad (51)$$

$$\frac{d\lambda}{dt} = \frac{1}{16\pi^2} \left[18\lambda^2 + 8\lambda y_t^2 - 8y_t^4 + \frac{\lambda M^2}{Z} \left(5 + \frac{(6\xi + 1)^2}{\omega} \right) + \frac{M^4 \xi^2}{2Z^2} \left(5 + \frac{(6\xi + 1)^2}{\omega^2} \right) \right] \quad (52)$$

$$\frac{d\xi}{dt} = \frac{1}{16\pi^2} \left[\left(\xi + \frac{1}{6} \right) \left\{ 4y_t^2 + 6\lambda + \frac{2M^2 \xi}{Z\omega} (3\xi + 2) \right\} - \frac{5M^2}{3Z} \xi \omega \right], \quad (53)$$

$$\frac{dy_t}{dt} = \frac{y_t}{16\pi^2} \left[5y_t^2 + \frac{15M^2}{8Z} \right], \quad (54)$$

where $t = \ln(\mu/\mu_0)$ (μ_0 is a reference scale) and $d/dt = \mu d/d\mu$. Here Z_φ and Z_ψ is the wave-functional renormalisation of scalar and fermion field respectively, while η_φ and η_ψ is the corresponding anomalous dimension. The beta-functions obtained here agree fully with [26, 27], while there is partial agreement with [23, 82–86]. For completeness we also include the running of gravitational couplings which has been taken from past literature [16, 78]. These are given by,

$$\frac{d}{dt} \left(\frac{Z}{M^2} \right) = -\frac{1}{16\pi^2} \left[\frac{133}{10} + \frac{N_s + 6N_f}{60} \right], \quad (55)$$

$$\frac{d}{dt} \left(\frac{Z\omega}{M^2} \right) = \frac{1}{16\pi^2} \left[\frac{5}{3} \omega^2 + 5\omega + \frac{5}{6} + 3N_s \left(\xi + \frac{1}{6} \right)^2 \right]. \quad (56)$$

We will be doing the RG analysis of the couplings and exploring the issue of unitarity later.

III. EFFECTIVE POTENTIAL

Here we compute the effective potential for the background scalar field φ which gets contributions not only from matter fields but also from gravitational sector.

To compute the effective potential for scalar, the background scalar field is taken to be constant. This is sufficient to compute the effective potential. The quantum gravitational fluctuations are considered around a flat background. The fermion fields are likewise decomposed into a constant background (which for simplicity is taken to be zero $\bar{\theta} = \theta = 0$) plus fluctuations. This simplifies the computation very much. As the ghost action doesn't depend on the background scalar field φ , therefore there is no contribution by the ghost to the effective potential, and hence will be ignored in the following. Once the full second variation of the action is performed, we have the hessian needed to compute the one-loop effective potential. This can be obtained directly from eq. (45) by putting background $\bar{R} = 0$ and replacing background covariant derivative with partial derivative. Being on flat background allows the freedom to work directly in momentum space.

Moreover, in flat space-time the transverse-traceless decomposition of $h_{\mu\nu}$ given in eq. (42) can be rewritten in an alternative form. In this new decomposition the field components σ and h of $h_{\mu\nu}$ are replaced by s and w . These new fields s and w are related to old ones in

the following manner

$$s = \frac{h - \square\sigma}{d}, \quad w = \frac{h + (d-1)\square\sigma}{d}. \quad (57)$$

The advantage of doing this transformation is to bring out the scalar mode which remains invariant under diffeomorphism transformation stated in eq. (8). The field s is therefore gauge invariant, while the field w is longitudinal. So the decomposition of $h_{\mu\nu}$ has two gauge-invariant components $h_{\mu\nu}^{TT}$ and s , with two longitudinal components $\hat{\xi}_\mu$ and w . Furthermore, on flat space-time one can also use the set of orthogonal projectors to project $h_{\mu\nu}$ on various components $h_{\mu\nu}^{TT}$, $\hat{\xi}_\mu$, s and w (see appendix B). In terms of new field variables, the hessian mentioned in eq. (45) can be rewritten (for $R = 0$) in a more transparent manner to see clearly the gauge-dependent and gauge-independent part. The hessian for $h_{\mu\nu}^{TT}$ and $\hat{\xi}_\mu$ remains same, while the mixing matrix of $\hat{\sigma}$, h and χ gets rotated due to field transformation stated in eq. (57). The new mixing between the field variables s , w and χ has a simplified structure. Moreover, this transformation of field variable is unaccompanied by any non-trivial jacobian in the path-integral. The one-loop effective potential is therefore obtained from a simplified hessian,

$$\begin{aligned} \Gamma^{(1)} = & \frac{(d+1)(d-2)i}{4} \text{Tr} \ln \left\{ -\frac{Z}{M^2} \square^2 - \frac{\xi}{2} \varphi^2 \square + \frac{\lambda}{4} \varphi^4 \right\} + \frac{(d-1)i}{2} \text{Tr} \ln \left\{ \frac{2}{\alpha} \square^2 + \frac{\lambda}{2} \varphi^4 \right\} \\ & + \frac{i}{2} \text{Tr} \ln \left[\det \begin{pmatrix} S_{ss} & S_{sw} & S_{s\phi} \\ S_{ws} & S_{ww} & S_{w\phi} \\ S_{\phi s} & S_{\phi w} & S_{\phi\phi} \end{pmatrix} \right] - i \text{Tr} \ln (i\gamma^\mu \partial_\mu - y_t \varphi), \end{aligned} \quad (58)$$

where the entries of the scalar mixing matrix are,

$$\begin{aligned} S_{ss} &= (d-1) \left[\frac{(d-2)Z\omega}{M^2} \square^2 + \frac{(d-2)}{2dM^2} \xi \varphi^2 \square - \frac{(d-3)\lambda}{8} \varphi^4 \right], \\ S_{sw} &= S_{ws} = -\frac{(d-1)\lambda}{8} \varphi^4, \quad S_{s\phi} = S_{\phi s} = -(d-1)\varphi [2\xi \square - \lambda \varphi^2], \\ S_{ww} &= \frac{2}{\alpha} \square^2 + \frac{\lambda}{8} \varphi^4, \quad S_{w\phi} = S_{\phi w} = -\lambda \varphi^3, \quad S_{\phi\phi} = -2\square - 6\lambda \varphi^2. \end{aligned} \quad (59)$$

From the entries of mixing matrix we clearly notice that S_{ss} , S_{sw} , $S_{s\phi}$ doesn't depend on gauge parameter. The only gauge dependence is in S_{ww} .

For a generic case with an arbitrary field variable, the one-loop hessian can be written in the form $(-\square - m^2)$ (where m^2 contain background field contributions and couplings). In this case the effective potential is given by the general formula

$$V_{\text{eff}}^{(1)} = \frac{d_s(m^2)^2}{64\pi^2} \left(\ln \frac{m^2}{\mu^2} - \frac{3}{2} \right), \quad (60)$$

where d_s is the factor coming due to the degrees of freedom of the field. The term $3/2$ in the bracket can be absorbed by rescaling μ^2 as $\bar{\mu}^2 = \mu^2 e^{3/2}$. By exploiting this generic formula one can write the contribution to the effective potential from the various field modes of the metric fluctuation field, the scalar and the fermion field. In the case for spin-2, the differential operator responsible for the contribution can be factored and has the form $(-\square - A_1 \varphi^2)(-\square - A_2 \varphi^2)$ where A_1 and A_2 are given by,

$$\begin{aligned} A_1 &= -2\sqrt{\pi} \left[\sqrt{f^2(4\pi f^2 \xi^2 + \lambda)} - 2\sqrt{\pi} f^2 \xi \right], \\ A_2 &= 2\sqrt{\pi} \left[\sqrt{f^2(4\pi f^2 \xi^2 + \lambda)} + 2\sqrt{\pi} f^2 \xi \right]. \end{aligned} \quad (61)$$

respectively. Here both A_1 and A_2 are dimensionless. It should be noted that for positive λ , A_1 is negative while A_2 are positive. If the sign of ξ is reversed, the roles of A_1 and A_2 gets interchanged. A negative A_1 is tachyonic in nature. This is a source of instability in the effective potential and will give imaginary contribution to the effective potential. Plugging $A_1\varphi^2$ and $A_2\varphi^2$ for the m^2 in the expression for the effective potential in eq. (60) and summing the two, we get the contribution of the spin-2 mode to the effective potential.

This imaginary piece though is an infrared effect. It is an indication that background chosen for doing the computation is not stable, and is a generic feature of gravity coupled with scalar field in flat space-time at zero temperature [19, 23]. This is same as the instability seen in the gas of graviton at finite temperature, an indication that flat space-time is unstable. This issue has been thoroughly investigated in past in [87, 88]. This kind of tachyonic mode will create issues with unitarity, but this one is different from the unitarity issue caused by the ghost of higher-derivative gravity, in the sense that the former is an IR problem and has no affect on the UV physics, while the later does affect the UV physics also. Since we are interested in sorting out the problem of unitarity caused by ghosts of higher-derivative, therefore we study only this by focusing on the real part of the effective potential, as the imaginary piece is relevant in IR and deals with tachyonic instability only. This is an important realisation as it decouples the two problems: (a) problem of unitarity caused by higher-derivative ghosts, and (b) problem of unitarity caused by tachyons. This paper deals with the former problem.

The contribution of the spin-0 mode is a bit complicated as it involves the scalar mixing matrix. We need to compute the determinant of this mixing matrix and then compute the effective potential of the operator so obtained from this matrix determinant. The operator obtained after matrix determinant is following,

$$-\square^3 - 3\varphi^2 \left[\frac{M^2\xi}{Z\omega} \left(\xi + \frac{1}{6} \right) + \lambda \right] \square^2 + \frac{M^2}{16Z\omega} \lambda(24\xi + 1)\varphi^4 \square - \frac{9M^2}{16Z\omega} \lambda\varphi^6. \quad (62)$$

This operator is a cubic polynomial in $-\square$ and will therefore have three roots. The nature of roots can be analysed using the discriminant Δ of the equation formed by putting the cubic polynomial in (62) to zero. We write

$$d_0 = 1, d_1 = -3\varphi^2 \left[\frac{M^2\xi}{Z\omega} \left(\xi + \frac{1}{6} \right) + \lambda \right], d_2 = -\frac{M^2}{16Z\omega} \lambda(24\xi + 1)\varphi^4, d_3 = -\frac{9M^2}{16Z\omega} \lambda\varphi^6, \\ \Delta = 18d_0d_1d_2d_3 - 4d_1^3d_3 + d_1^2d_2^2 - 4d_0d_2^3 - 27d_0^2d_3^2. \quad (63)$$

If $\Delta > 0$ then all roots are real, if $\Delta = 0$ then there is a multiple root, and $\Delta < 0$ then roots are complex. The operator in eq. (62) can be factorised as $(-\square - B_1\varphi^2)(-\square - B_2\varphi^2)(-\square - B_3\varphi^2)$ where B_1, B_2 and B_3 are dimensionless. As the product of roots $B_1B_2B_3$ is positive and $B_1B_2 + B_2B_3 + B_3B_1$ is negative, therefore this will imply that when $\Delta > 0$ then two roots will be negative. If $\Delta = 0$, then there is a multiple root with negative sign. In the case when $\Delta < 0$ there is a pair of complex conjugate root with negative real part and a positive real root. The cases with $\Delta \geq 0$ has roots carrying negative sign, while for $\Delta < 0$ the complex conjugate pair has a negative real part. In all these cases the roots can be written as

$$B_1 = a, B_2 = -re^\theta, B_3 = -re^{-\theta}. \quad (64)$$

In the case when $\Delta > 0$, θ is positive and real, in $\Delta = 0$ case $\theta = 0$, while in $\Delta < 0$ case θ is imaginary. The factor of -1 in the parametrisation of roots can also be exponentiated

as $e^{i\pi}$. This factor is the source of tachyonic instability and will give rise to an imaginary contribution in the effective potential. This is similar to the instability caused in spin-2 case and is an indication that flat space-time is not a true vacuum [87, 88]. The contribution to the effective potential from the scalar sector is now easily computed using the generalised expression given in eq. (60). This is done by replacing m^2 in eq. (60) with $B_1\varphi^2$, $B_2\varphi^2$ and $B_3\varphi^2$, and summing all together. Using the parametrisation for the roots written in eq. (64) and employing the properties of exponential functions, one can write the effective potential in simple terms³.

The contribution of the fermions needs to be done in a different manner. It arises from $-i\text{Tr}\ln(i\gamma^\mu\partial_\mu - y_t\varphi)$. This can be written in an alternative form by squaring the operator and by making use of the gamma-matrix properties. This then become $-i/2\text{Tr}\ln(-\square - y_t^2\varphi^2)$. Then using the generalised expression in eq. (60) one gets the contribution for the fermions. The full effective potential involves the tree-level contributions plus the quantum corrections. The one-loop RG improved full effective action is then given by,

$$V_{\text{eff}}^{(1)} = \frac{\lambda(t)}{4}Z_\phi^4(t)\varphi^4 + \frac{Z_\phi^4(t)\varphi^4}{64\pi^2} \left[5 \sum_{i=1}^2 |A_i|^2 \ln \frac{|A_i|\varphi^2}{\bar{\mu}^2} + B_1^2 \ln \frac{B_1\varphi^2}{\bar{\mu}^2} + 2r^2 \cosh(2\theta) \ln \frac{r\varphi^2}{\bar{\mu}^2} + 2r^2\theta \sinh(2\theta) - y_t^4 \ln \frac{y_t^2\varphi^2}{\bar{\mu}^2} + \frac{iZ_\phi^4(t)\varphi^4}{64\pi} \{5|A_1|^2 + 2r^2 \cosh(2\theta)\} \right], \quad (65)$$

where A_i 's, B_1 , r and θ are dimensionless and RG-time t dependent. When $\theta \rightarrow i\theta$, $\cosh(2\theta) \rightarrow \cos(2\theta)$ and $\sinh(2\theta) \rightarrow i\sin(2\theta)$, thereby preventing the switching between real and imaginary part.

In the following we will study the real part of the effective potential. We ignore the imaginary part, as the imaginary part arises from the tachyonic modes of theory and is relevant in IR. We are interested in investigating unitarity issues caused by higher-derivatives ghosts. It should be noticed that the effective potential still posses the \mathbf{Z}_2 symmetry, as $\varphi^2 = 0$ is an extrema. But due to radiative corrections the real part of quantum corrected effective potential might develop a vacuum expectation value (VeV) away from zero.

IV. SYMMETRY BREAKING

Due to RG corrections a VeV is generated in the effective potential, which then becomes the new vacuum. The original $\varphi^2 = 0$ vacuum becomes unstable under RG corrections and the field migrates to the new vacuum which occur at $\varphi^2 = \kappa^2$. It is given by,

$$\left. \frac{d}{d\varphi^2} \text{Re}(V_{\text{eff}}) \right|_{\varphi^2=\kappa^2} = 0. \quad (66)$$

At the tree level our original action of the theory is scale-invariant and there is no mass-parameter to begin with. However the mass parameter enters the system via RG running thereby breaking scale-invariance. The effective potential so generated not only breaks scale invariance but also breaks the \mathbf{Z}_2 symmetry. The generation of VeV consequently gives

³ The discriminant Δ depends on RG time t , and during the RG evolution can change sign, thereby implying that during the RG evolution θ can switch from real to imaginary and viceversa.

mass to scalar and fermion fields. It also generates an effective Newton's constant, beside generating newer interactions. The generated mass and Newton's coupling can be expressed in terms of VeV κ^2 and all the other couplings as

$$m_s^2 = \frac{3}{2}\lambda\kappa^2, \quad m_f = y_t\kappa, \quad G^{-1} = 8\pi\xi\kappa^2. \quad (67)$$

The generation of mass and Newton's constant makes the propagators for various fields massive. In particular the graviton propagator after the symmetry breaking is following,

$$D^{\mu\nu,\alpha\beta} = 16\pi G \cdot \left[\frac{(2P_2 - P_s)^{\mu\nu,\alpha\beta}}{q^2 + i\epsilon} + \frac{(P_s)^{\mu\nu,\alpha\beta}}{q^2 - M^2/\omega + i\epsilon} - \frac{2(P_2)^{\mu\nu,\alpha\beta}}{q^2 - M^2 + i\epsilon} \right], \quad (68)$$

where now G is the induced Newton's constant and is defined using eq. (67). The masses M^2 and M^2/ω are given by

$$M^2 = 8\pi f^2 \cdot \xi\kappa^2, \quad \frac{M^2}{\omega} = 8\pi \frac{f^2}{\omega} \xi\kappa^2. \quad (69)$$

The interesting thing about the generation of Newton's constant is that now as the propagator becomes massive, so there is a spin-2 massive ghost that appears in the system, which in the original theory was massless. In the original theory we cannot do the partial-fraction trick in the $h_{\mu\nu}$ propagator, which is possible in the broken phase due the induced Newton's constant G . Not only the spin-2 ghost becomes massive but also the scalar mode acquires mass through symmetry breaking. We call this massive scalar mode 'Riccion'. It should be pointed out that if we had taken ξ to be negative, then there will be tachyons in the broken phase. So the presence of higher-derivatives terms and requiring no tachyons to be generated in broken phase fixes the sign of ξ . This also generates right sign for induced Newton's constant. The sign of various couplings in the broken phase is then in accordance with the sign of parameters taken in [5, 6].

At this point we compare the propagator of metric fluctuation written in eq. (17) with the one written in eq. (68). The former is before symmetry breaking while the later is after symmetry breaking. The former has no mass, while later contains masses. Although the appearances of the two are different one should however be careful while counting the propagating degrees of freedom in the two. In the later case (broken phase) it is easy to count: two massless graviton modes, five massive-tensor ghost modes and one massive scalar mode, thereby making eight propagating degrees of freedom. In the former case (unbroken phase) one should count carefully. The pure $C_{\mu\nu\rho\sigma}^2$ -gravity has six massless propagating degrees of freedom [89, 90]. For pure R^2 gravity, the theory two massless propagating degrees of freedom as the linearised field equation $(\partial_\mu\partial_\nu - \eta_{\mu\nu}\square)\square h = 0$ shows to have fourth-order time derivatives. Thereby totalling the degrees of freedom in unbroken phase to be eight. This implies that the propagating degrees of freedom in both phases is same, except in broken phase some of the modes acquire mass due to symmetry-breaking.

The generation of mass for the spin-2 ghost and scalar-mode gives us a hope to investigate unitarity by using the criterion stated in [3, 5–8]. In the RG improved effective potential the VeV has t -dependence. This arises because at each energy scale the effective potential has a VeV. This translates into t -dependence of VeV. The RG running of VeV depends on the running of the other couplings in a complicated manner. This running of VeV then translates into running of generated Newton's constant. The running of the VeV κ^2 can

be computed using the expression of the real part of effective potential given in eq. (65). When $\varphi^2 = \kappa^2$, then we are at the minima. The minima condition written in eq. (66) then translates into following,

$$\left. \frac{d}{d\varphi^2} \text{Re}(V_{\text{eff}}) \right|_{\varphi^2=\kappa^2} = Z_\phi^4(t) \kappa^2 \left[\frac{\lambda(t) + \rho_1(t)}{2} + \rho_2(t) + \rho_1(t) \ln \frac{\kappa^2(t)}{\bar{\mu}^2} \right] = 0. \quad (70)$$

where,

$$\begin{aligned} \rho_1(t) &= \frac{1}{32\pi^2} \left\{ 5 \sum_{i=1}^2 A_i^2 + B_1^2 + 2r^2 \cosh(2\theta) - y_t^4 \right\}, \\ \rho_2(t) &= \frac{1}{32\pi^2} \left[5 \sum_{i=1}^2 A_i^2 \ln|A_i| + B_1^2 \ln B_1 + 2r^2 \cosh(2\theta) \ln r + 2r^2 \theta \sinh(2\theta) - y_t^4 \ln y_t^2 \right] \end{aligned} \quad (71)$$

As $\kappa^2 \neq 0$ and $Z_\phi \neq 0$ therefore these overall factors goes away and the residual condition simplifies to the expression in the square bracket written in eq. (70). As $\kappa^2(t)/\bar{\mu}^2$ is dimensionless, we call it $K(t)$. One can then directly solve for $K(t)$ using eq. (70) in terms of all couplings of theory. This also gives the flow of K which is generated due to the flow of various couplings present in the theory. We however take a t -derivative of the expression in the square-bracket of eq. (70) to compute the beta-function of the $K(t)$. This is needed in checking and locating extrema of $K(t)$. Such extrema are crucial points as will be seen later.

$$\frac{dK(t)}{dt} = -\frac{K(t)}{\rho_1(t)} \left[\frac{\lambda'(t) + \rho_1'(t)}{2} + \rho_2'(t) + \rho_1'(t) \ln K(t) \right]. \quad (72)$$

This is a linear first order differential equation for the $\ln K(t)$. Plugging the running of various couplings from eq. (52, 53, 54, 55, 56) in RHS of eq. (72) we get the beta function of $K(t)$. This will be a very complicated function of various couplings. Using the running of $K(t)$ we can compute the running of the effective Newton's constant by exploiting the expression for induced G mentioned in eq. (67). This is given by,

$$\frac{dG(t)}{dt} = -G(t) \left[\frac{1}{\xi(t)} \frac{d\xi(t)}{dt} + \frac{1}{K(t)} \frac{dK(t)}{dt} + 2 \right]. \quad (73)$$

In order to investigate the issues of unitarity caused by higher-derivative we consider the following combination M^2/μ^2 . We first note that this is

$$\frac{M^2}{\mu^2} = 8\pi e^{3/2} f^2(t) \cdot \xi(t) \cdot K(t). \quad (74)$$

Taking t -derivative of this yields,

$$\frac{d}{dt} \ln \frac{M^2}{\mu^2} = \frac{1}{f^2} \frac{df^2}{dt} + \frac{1}{\xi(t)} \frac{d\xi(t)}{dt} + \frac{1}{K(t)} \frac{dK(t)}{dt}. \quad (75)$$

Similarly the expression for induced $M^2/\omega\mu^2$ is,

$$\frac{M^2}{\omega\mu^2} = 8\pi e^{3/2} \frac{f^2(t)}{\omega(t)} \cdot \xi(t) \cdot K(t), \quad (76)$$

and the RG flow of this combination is given by,

$$\frac{d}{dt} \ln \frac{M^2}{\omega \mu^2} = \frac{1}{f^2} \frac{df^2}{dt} - \frac{1}{\omega(t)} \frac{d\omega(t)}{dt} + \frac{1}{\xi(t)} \frac{d\xi(t)}{dt} + \frac{1}{K(t)} \frac{dK(t)}{dt}. \quad (77)$$

The generation of VeV also induce masses for the scalar and the fermion fields, which is mentioned in eq. (67). Due to the running of VeV, these masses inherits a running. Then to investigate whether these fields are physically realisable or not, we consider the flow of combinations m_s^2/μ^2 and m_f^2/μ^2 . The running of these combinations is given by,

$$\frac{d}{dt} \ln \frac{m_s^2}{\mu^2} = \frac{1}{\lambda(t)} \frac{d\lambda(t)}{dt} + \frac{1}{K(t)} \frac{dK(t)}{dt}, \quad \frac{d}{dt} \ln \frac{m_f^2}{\mu^2} = \frac{2}{y_t(t)} \frac{dy_t(t)}{dt} + \frac{1}{K(t)} \frac{dK(t)}{dt}. \quad (78)$$

V. UNITARITY PRESCRIPTION

In this section we dictate the algorithm to choose the set of initial conditions for which the theory will have a unitary flow. We start by analysing the RG equations given in eq. (52, 53, 54, 55, 56). The first thing we do is to extract the running ω using the eq. (55 and 56). This is given by,

$$\frac{d\omega(t)}{dt} = \frac{f^2}{\pi} \left[\frac{5}{3} \omega^2 + \left\{ \frac{183}{10} + \frac{N_s + 6N_f}{60} \right\} \omega + \frac{5}{6} + 3N_s \left(\xi + \frac{1}{6} \right)^2 \right]. \quad (79)$$

From this running we notice that as the RHS is always positive therefore ω is a monotonically increasing function of t . In [5–8] it was shown that in order to avoid tachyonic instability, we should demand that $\omega \geq 0$. Here in the present scale-invariant theory we should demand the same. This is done in order to prevent the occurrence of tachyons in the broken phase. For every value of ξ , ω will have two fixed points.

$$\omega_{1,2} = -\frac{1}{40} \left[221 \mp \sqrt{47961 - 960\xi - 2880\xi^2} \right]. \quad (80)$$

ω_1 is repulsive while ω_2 is attractive. For ξ small both these fixed points lie in the unphysical tachyonic regime. For large ξ the fixed points are complex conjugate with negative real part. Since ω is monotonically increasing with t , therefore one can alternatively study the RG flows of various parameters in terms of ω . Prevention of tachyonic instability restricts ω to lie between zero and infinity. This then serves as a good candidate in terms of which the the RG flows can be analysed. In [5–8] the RG flows were studied in terms of ω .

The crucial problem in overcoming the issue of unitarity is to choose the right set of initial conditions so that throughout the RG evolution the flow remains unitary in the sense that the ghost mass remains always above the energy scale, and the effective potential doesn't develop any further instability (other than the ones already present). To prevent the occurrence of this instability requires that the coupling λ remains positive throughout the RG flow (as negative λ will result in tachyonic instability for scalar field ϕ). This particularly depends on the choice of initial condition for yukawa coupling. If the yukawa coupling is above a certain threshold then λ becomes negative too soon during the RG evolution, making the effective potential unstable. In standard model of particle physics this is an important instability problem where the electroweak vacuum becomes metastable [91] (see references therein). In

present case of scale invariant gravity, we have freedom to explore the set of initial conditions which will give unitary evolution. So we just consider those domains where this instability can be avoided.

In [5–8] it was observed that the RG evolution of M^2/μ^2 is such that its flow has a unique minima. This was a crucial feature which allowed us to seek those RG trajectories for which this minima is above unity. These RG trajectories are the ones for which the flow is unitary (massive tensor mode is not physically realisable). In the present case of gravity being induced from scale-invariant theory we seek a similar behaviour of induced M^2/μ^2 , where now M^2 is given by eq. (69), and the flow of M^2/μ^2 is given in eq. (75). The flow of M^2/μ^2 is much complicated in the present case and it is difficult to give a rigorous analytic proof that there exist a minima in the RG evolution of M^2/μ^2 . From various numerical investigations we realised that a minima does exist in the evolution of induced M^2/μ^2 . We choose this minima to be our reference point and choose the initial conditions at this point for all other couplings. The appearance of a minima in the flow induced M^2/μ^2 implies that at this minima the beta-function of induced M^2/μ^2 will vanish,

$$\frac{1}{f^2} \frac{df^2}{dt} \Big|_{t=t_*} + \frac{1}{\xi(t)} \frac{d\xi(t)}{dt} \Big|_{t=t_*} + \frac{1}{K(t)} \frac{dK(t)}{dt} \Big|_{t=t_*} = 0. \quad (81)$$

Plugging the RG-flows of various coupling in this, will result in a condition satisfied by all the couplings of theory at this minima. This will act as a constraint in choosing some of the initial parameters. We first choose the value of M^2/μ^2 at this point, we call it ρ_* . We require $\rho_* > 1$.

$$\frac{M^2}{\mu^2} \Big|_{t=t_*} = 8\pi e^{3/2} f_*^2 \cdot \xi_* \cdot K_* = \rho_* > 1, \quad (82)$$

where f_*^2 , ξ_* and K_* are initial values of f^2 , ξ and K respectively. The imposition of this constraint makes sure that the mass of the spin-2 ghost mode remains above the running energy scale. This will imply that one of the three unknowns f_*^2 , ξ_* and K_* can be expressed in terms of other two. We choose to write K_* in terms of f_*^2 and ξ_* . At this point we also choose $f_*^2 \ll 1$. Now the left unknowns are λ_* , $(y_t)_*$, ω_* and ξ_* . In order to choose the matter couplings λ_* we use our knowledge of non-gravitational system. In such system the running λ always hits the Landau pole if the initial value of yukawa coupling is below certain threshold, beyond which λ becomes negative leading to instability. We accordingly choose $\lambda_* \lesssim 0.1$.

At this point we analyse the beta-function for the coupling ξ . In this theory we have the freedom to choose ξ to be very large ($\gtrsim 10$). This is primarily because in the perturbation theory the coupling strength of vertex containing n -gravitons and two scalars is $\sim \xi(\sqrt{f^2})^n$ and $\sim \xi(\sqrt{f^2/\omega})^n$. Since $f^2 \ll 1$, so this give us freedom to choose ξ to be very large while still being in the realm of perturbation theory⁴. For ξ large the beta-functions of various coupling acquires a simplified form. Although the beta functions become simplified but still they are complicated enough that it requires the analysis to be done numerically. We tend to explore numerically this regime of parameters.

We choose to work in regime where $-\Delta/\varphi^6 = \epsilon \ll 1$, where Δ is the discriminant mentioned in eq. (63). In this regime there will one positive root for $-\square$ and a complex

⁴ In the case on Einstein-Hilbert gravity with only Newton's constant G , the coupling strength is $\xi(\sqrt{G})^n$ for a vertex containing n -gravitons and two scalars.

conjugate pair with negative real part. Under the RG flow Δ/φ^6 will also run. We choose the initial parameters in such a way so that at the initial point $\epsilon \ll 1$. By reversing this argument we say that we start with $\epsilon \ll 1$ and solve for the initial parameters under this constraint. This fixes the initial value problem completely. With the chosen $f_*^2 \ll 1$ ($\lesssim 10^{-6}$), $\rho_* > 1$, $\lambda_* \lesssim 0.1$ and $\xi_* \gg 1$ ($\gtrsim 10^2$), we use the constraint dictated by $\epsilon \ll 1$ to solve for ω_* . From the four different solution for ω_* , we choose the one which real and positive (to avoid tachyons)⁵. Knowledge of ξ_* gives the initial value of K_* by using the relation given in eq. (82). We then plug these into the minima constraint given in eq. (81). This constraint contains the yukawa coupling in quadratic form, and therefore on solving gives two equal and opposite values for y_{t*} . One can choose either of the sign of yukawa coupling for the initial condition. The flow of all the other couplings doesn't depend on this sign. Once the initial parameters are known we can solve the RG flows and compute the flow of induced M^2/μ^2 to see if it remains above unity throughout the RG evolution.

VI. NUMERICAL ANALYSIS

We tried several possible values of various parameters in order to see how the flows are for various initial conditions, and did the analysis case by case systematically.

A. Fixed λ_*

We first considered case with fixed λ_* , while we took different values for f_*^2 , and for each f_*^2 we explored a range of ξ_* . Throughout this we took $\rho_* = 1.5$ (there is nothing special about this number, as long as long as $\rho_* > 1$). We considered three different values for $f_*^2 = 10^{-6}$, 10^{-7} and 10^{-8} . We have freedom over the choice of $-\Delta_*/\varphi^6 = \epsilon$. It is seen that with f_*^2 fixed, when ϵ is made smaller, then ω_* increases. However the y_{t*} obtained first decreases to a minima before rising again and becoming stable. We choose ϵ near this minima, so that we have more number of e-folds in the RG flows. It turns out that for each value of f_*^2 the position of occurrence of this minima will be different. For smaller f_*^2 , the minima occurs at a smaller value of ϵ . Thus for $f_*^2 = 10^{-6}$, 10^{-7} and 10^{-8} , the minima for ϵ occurs around 10^{-12} , 10^{-15} , and 10^{-16} respectively. We consider these cases in succession.

The number of e-folds from the Planck's time to current galactic scale is ~ 130 . This stands then as another guiding principle to choose set of initial parameters. It is noticed that when f_*^2 is made more smaller then the allowed upper value of ξ_* (which is chosen so that we have $\gtrsim 100$ e-folds) increases. This can be understood by considering the strength of vertices. For vertex containing one graviton leg and two scalar leg, the interaction strength $\sim \xi\sqrt{f^2}$. Demanding perturbation theory to remain valid implies $\xi_*\sqrt{f_*^2} \lesssim 1$, which explains the behaviour. We keep ξ_* large so that there is sufficient communication between the matter and gravity sector. In table I we tabulate our findings for $f_*^2 = 10^{-6}$, 10^{-7} and 10^{-8} .

We then plot the flows of various parameters for the choice of initial parameters written in table I. Each flow is interesting to analyse. The flow of the coupling ξ for various choices of the initial conditions is shown in figure 5. The plot shown in figure 5 is for $f_*^2 = 10^{-8}$

⁵ It is noticed that if $\epsilon < 0$, then all solutions for ω_* will be negative and will lie in unphysical tachyonic regime. This knowledge also demands to take $\epsilon > 0$.

$f_*^2 = 10^{-6}$				$f_*^2 = 10^{-7}$				$f_*^2 = 10^{-8}$			
ξ_*	$\omega_* \times 10^{-4}$	y_{t*}	T_r	ξ_*	$\omega_* \times 10^{-6}$	y_{t*}	T_r	ξ_*	$\omega_* \times 10^{-6}$	y_{t*}	T_r
1	3.0536	0.4522	~ 215	10^2	3.0536	0.4536	$\gtrsim 235$	10^2	3.0536	0.4522	$\gtrsim 230$
10	3.0536	0.4532	~ 215	5×10^2	3.0536	0.4543	$\gtrsim 267$	10^3	3.0536	0.4532	$\gtrsim 212$
10^2	3.0549	0.4543	$\gtrsim 217$	10^3	3.0537	4546	~ 437	10^4	3.0549	0.4542	$\gtrsim 235$
5×10^2	3.0869	0.4562	$\gtrsim 305$	2×10^3	3.0542	0.4551	~ 250	5×10^4	3.0869	0.4562	$\gtrsim 305$
10^3	3.1840	0.4603	~ 356	5×10^3	3.0569	0.4561	~ 120	10^5	3.1840	0.4603	~ 356
5×10^3	5.3737	0.5355	~ 60	10^4	3.0669	0.4587	~ 72	5×10^5	5.3736	0.5355	~ 58

TABLE I: Initial values for the various coupling parameters. These are for $f_*^2 = 10^{-6}$, 10^{-7} and 10^{-8} . We took $\lambda_* = 0.1$ and $\rho_* = 1.5$. Here for three different values of f_*^2 we took $\epsilon = 10^{-12}$, 10^{-15} and 10^{-16} . As ξ_* increase, the value of ω_* and y_{t*} increase. The number of e-folds tend to decrease as ξ_* increases. For smaller ξ_* the reason we see less e-folds is due to numerical precision of machine.

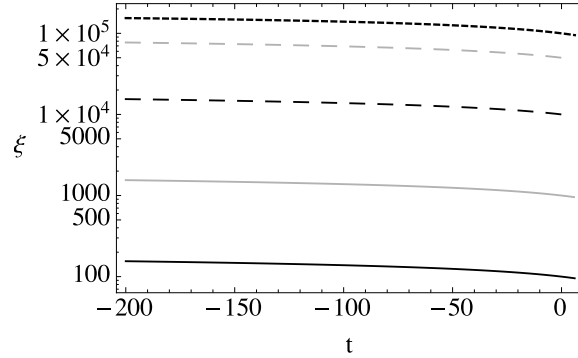


FIG. 5: Running of coupling ξ for various values of initial conditions $\xi_* = 10^2$ (black solid line), 10^3 (grey solid line), 10^4 (big dashed black line), 5×10^4 (big dashed grey line) and 10^5 (small dashed black line). For these flows we took $f_*^2 = 10^{-8}$, $\lambda_* = 0.1$, $\rho_* = 1.5$ and $\epsilon = 10^{-16}$.

only, for other values we observe similar qualitative behaviour which will not be shown here. From the running of ξ shown in figure 5 we notice that the parameter ξ runs to smaller values in the UV regime. This might be an indication of the possible existence of an UV stable fixed point, but it is hard to give a robust answer in this paper. This however can be justified by looking at the beta-function of ξ given in eq (53) whose *r.h.s.* can be seen to vanish for a certain choice of coupling parameters.

The flow of matter couplings λ and y_t for various initial conditions is shown in left and right of figure 6 respectively. For smaller values of ξ_* the flow of these couplings remain almost same, while deviations are seen for large ξ_* . This is again plotted for $f_*^2 = 10^{-8}$, while for other values of f_*^2 qualitatively similar behaviour is seen. In the UV the flow of λ is seen to bend and run toward smaller values, which is caused by the yukawa coupling.

The flow of the VeV induces a flow in the Newton's constant. The flow of the induced Newton's constant for various initial conditions is shown in figure 7. The induced Newton's constant goes to zero in the UV and in IR. In UV it is seen to go to zero at a finite energy scale. This is similar to the flow of Newton's constant observed in [5–8], where the original action was not scale-invariant and contained Einstein-Hilbert piece in the higher-derivative action. This is somewhat interesting to note. Again this is just a numerical observation and not a rigorous analytic argument. By varying the value of f_*^2 we notice that the qualitative features of the graph remains same.

Figure 8 shows the flow of parameters M^2/μ^2 and $M^2/\omega\mu^2$ in left and right respectively.

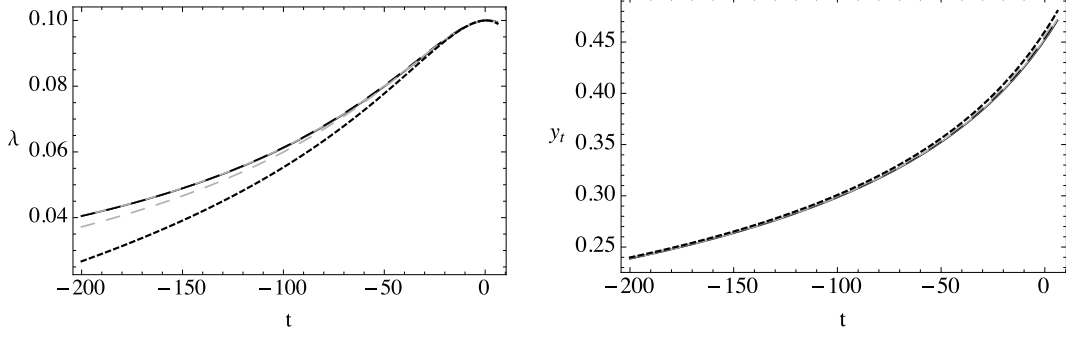


FIG. 6: Running for matter couplings λ and y_t in left and right respectively. These are plotted for $f_*^2 = 10^{-8}$, $\lambda_* = 0.1$, $\rho_* = 1.5$ and $\epsilon = 10^{-16}$. We considered the following initial conditions for $\xi_* = 10^2$ (black solid line), 10^3 (grey solid line), 10^4 (big dashed black line), 5×10^4 (big dashed grey line) and 10^5 (small dashed black line).

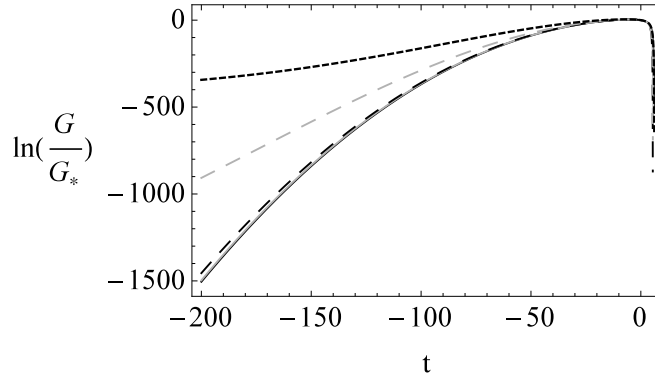


FIG. 7: The flow of the induced Newton's constant. Here we plot $\ln(G/G_*)$ for the case $f_*^2 = 10^{-8}$, $\lambda_* = 0.1$, $\rho_* = 1.5$ and $\epsilon = 10^{-16}$. The flow is computed for five different values of $\xi_* = 10^2$ (black solid line), 10^3 (grey solid line), 10^4 (big dashed black line), 5×10^4 (big dashed grey line) and 10^5 (small dashed black line). Both in UV and IR the flow goes very close to zero.

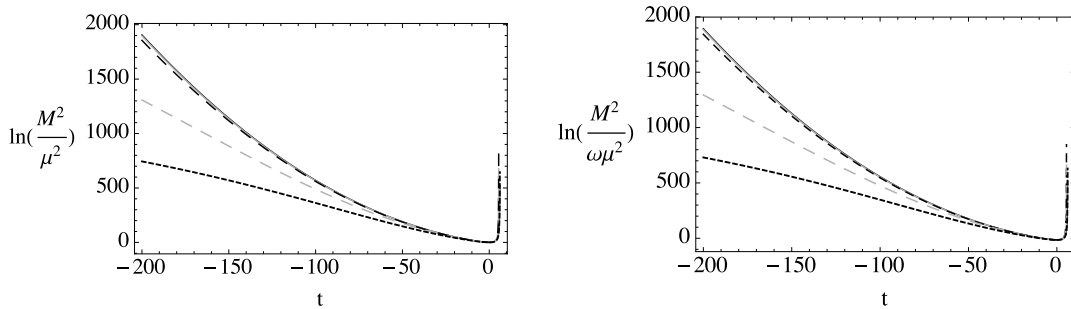


FIG. 8: The running of induced $\ln(M^2/\mu^2)$ and $\ln(M^2/\omega\mu^2)$ for the case $f_*^2 = 10^{-8}$, $\lambda_* = 0.1$, $\rho_* = 1.5$ and $\epsilon = 10^{-16}$. The flow is computed for five different values of $\xi_* = 10^2$ (black solid line), 10^3 (grey solid line), 10^4 (big dashed black line), 5×10^4 (big dashed grey line) and 10^5 (small dashed black line). In all cases it is seen that the flow has a minima. If the flow is such that we have $M^2/\mu^2 > 1$ throughout the flow, then this spin-2 ghost mode never goes on-shell, and theory satisfies unitarity.

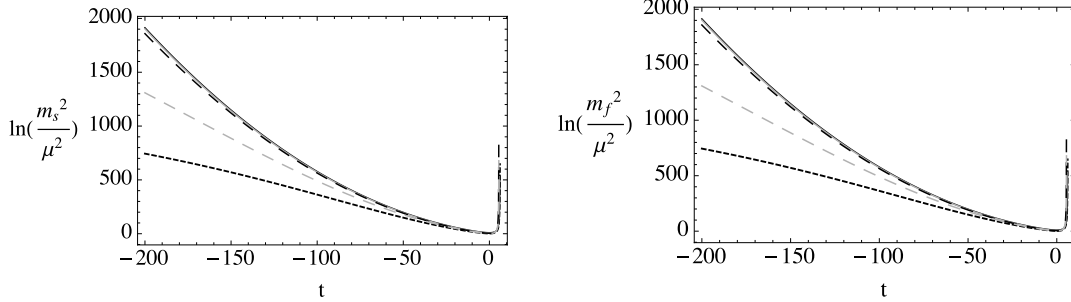


FIG. 9: The running of induced $\ln(m_s^2/\mu^2)$ and $\ln(m_f^2/\mu^2)$ for the case $f_*^2 = 10^{-8}$, $\lambda_* = 0.1$, $\rho_* = 1.5$ and $\epsilon = 10^{-16}$. The flow is computed for five different values of $\xi_* = 10^2$ (black solid line), 10^3 (grey solid line), 10^4 (big dashed black line), 5×10^4 (big dashed grey line) and 10^5 (small dashed black line). In all cases it is seen that the flow has a minima. If throughout the flow both $m_s^2/\mu^2 > 1$ and $m_f^2/\mu^2 > 1$ then both of them never go on-shell.

The flow of M^2/μ^2 is such that it is always above unity ($M^2/\mu^2 > 1$). This means that the propagator of metric fluctuation after symmetry breaking doesn't witness the ghost pole, as the problematic ghost mode is never realised and never goes on-shell. We observe this to happen for a large domain of coupling parameter space. A similar running of the parameter M^2/μ^2 was also observed in [5–8], and was used to establish unitarity criterion for the higher-derivative gravity. The flow of the parameter $M^2/\omega\mu^2$ is different from the one observed in [5–8], where a monotonic behaviour was seen. In the present case we see a convex structure with a single minima in the flow. If we demand that $M^2/\mu^2|_* > 1$, then it doesn't imply that $M^2/\omega\mu^2|_* > 1$. However the reverse is always true *i.e.* $M^2/\omega\mu^2|_* > 1$ implies $M^2/\mu^2|_* > 1$. By choosing ρ_* to be large enough one can make the scalar mode also physically unrealisable.

We then consider the induced masses in the matter sector and consider the flow of combinations m_s^2/μ^2 and m_f^2/μ^2 , where m_s and m_f is given in eq. (67). The induced RG running of them is shown in figure 9. The running of these is interesting in the sense that both of them has a minima. The value at the minima depends crucially on the initial parameters chosen to make the flow unitary. If we choose ρ_* large enough then it is possible that flow of m_s^2/μ^2 and m_f^2/μ^2 will be such that the scalar and fermion will never be realised during the whole RG flow, and they never go on-shell. In that sense they affect the theory indirectly and only gravitationally but they never go on-shell.

B. Fixed f_*^2

In the previous subsection the case with fixed λ_* was investigated. It is worth checking the robustness of the qualitative features when other parameters are varied. One particular important parameter is the λ_* . It is important to see how the situation changes when λ_* is increased. For this we fix the value of $f_*^2 = 10^{-8}$, $\xi_* = 10^5$, $\rho_* = 1.5$. We took a range of value of $\lambda_* = 0.2, 0.25, 0.3, 0.35$ and 0.45 . Although the qualitative features are same but there are minor differences. In each case we always witness that the running M^2/μ^2 has a minima, and the flow is always above unity. This further establishes that there always exist a minima in the flow of induced M^2/μ^2 , and it also implies that by choosing right set of

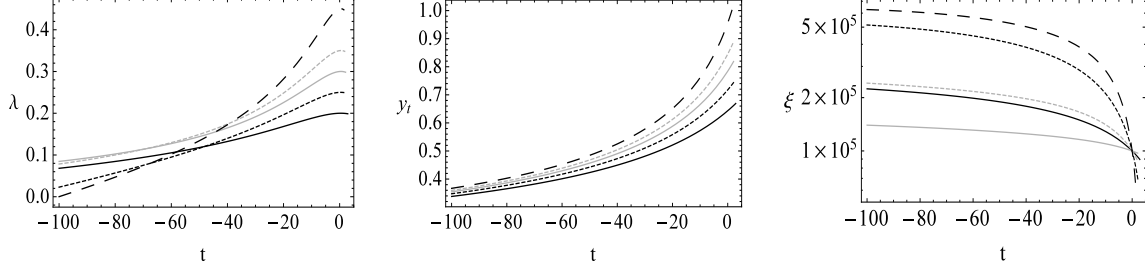


FIG. 10: Running for couplings λ , y_t and ξ in left, centre and right respectively. These are plotted for $f_*^2 = 10^{-8}$, $\lambda_* = 0.2$ (black solid line), 0.25 (black short-dashed line), 0.3 (grey solid line), 0.35 (grey short-dashed line) and 0.45 (black long-dashed line). We took $\rho_* = 1.5$ and $\xi_* = 10^5$.

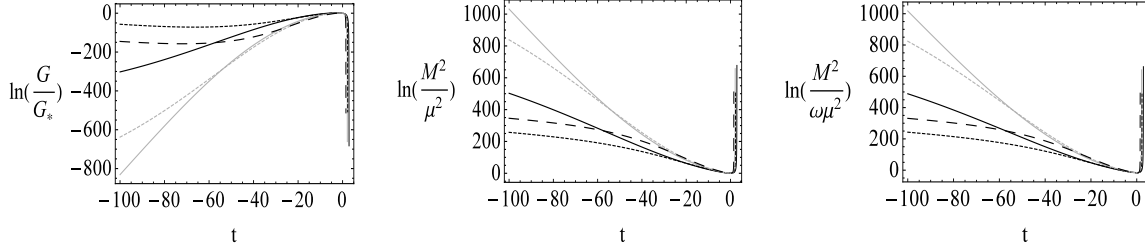


FIG. 11: The running of induced $\ln(G/G_*)$, $\ln(M^2/\mu^2)$ and $\ln(M^2/\omega\mu^2)$ in left, centre and right respectively. These are plotted for $f_*^2 = 10^{-8}$, $\lambda_* = 0.2$ (black solid line), 0.25 (black short-dashed line), 0.3 (grey solid line), 0.35 (grey short-dashed line) and 0.45 (black long-dashed line). We took $\rho_* = 1.5$ and $\xi_* = 10^5$.

initial condition it is possible to make the massive tensor ghost innocuous.

As the system contain a mixture of several coupling which are all evolving in different manner, therefore the dynamics of system is rich and interesting. This becomes more apparent when we plot the running of various parameters. The flow of λ , y_t and ξ is shown in figure 10. These flows are very much similar to the ones shown for fixed λ_* in the previous sub-section. It is seen that as λ_* is increased the flow of ξ decrease more sharply in the UV, and in IR the flow goes to higher values, even though starting point is same. The running of yukawa coupling is simple, in the sense that when λ_* increases, so does y_{t*} and accordingly the whole RG trajectory for yukawa coupling. The flow of λ is interesting. For higher λ_* , ξ flows to higher values in the IR. This makes the λ to run faster toward zero in the IR. In the UV the RG trajectories for λ has self-similarity.

The flow of G , M^2/μ^2 and $M^2/\omega\mu^2$ is shown in left, centre and right respectively in figure 11. The qualitative behaviour is the same in the sense that the induced Newton's constant goes to zero in the UV at a finite energy scale. It goes to zero in the IR. The RG flows for M^2/μ^2 and $M^2/\omega\mu^2$ have same qualitative features, and tensor ghost is physically unrealisable even when we increase λ_* . Choosing appropriate ρ_* will make the Riccion also physically unrealisable. The RG flow of Riccion mass is different from the one seen in [5–8]. The flow of induced masses in the matter sector has similar qualitative features and is shown in figure 12.

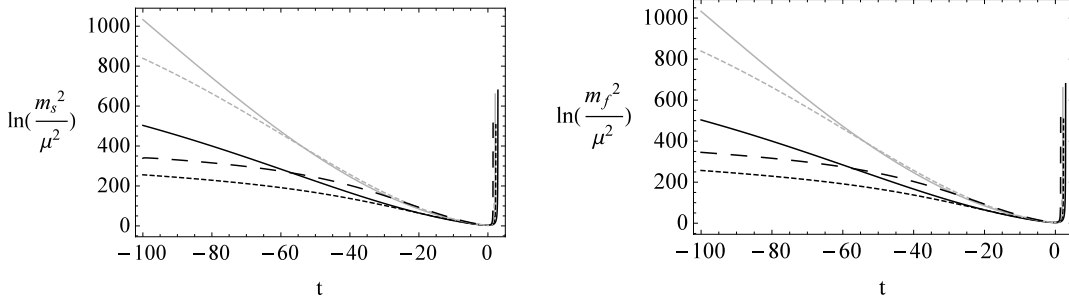


FIG. 12: The running of induced $\ln(m_s^2/\mu^2)$ and $\ln(m_f^2/\mu^2)$ in the left and right respectively. These are plotted for $f_*^2 = 10^{-8}$, $\lambda_* = 0.2$ (black solid line), 0.25 (black short-dashed line), 0.3 (grey solid line), 0.35 (grey short-dashed line) and 0.45 (black long-dashed line). We took $\rho_* = 1.5$ and $\xi_* = 10^5$. Choosing appropriate ρ_* it is possible to make the both the scalar and fermion unrealisable.

C. Fixing Planck's scale

The renormalisation group invariance insures that the flow of couplings doesn't depend on the reference point μ_0 . This gave us freedom to choose the reference point without any conditions. As a result for sake of convenience we choose it to be the point where the flow of M^2/μ^2 has a minima, where the initial conditions for the flow are imposed. However an interesting thing to ask is to how to relate it with the phenomenology? In the sense how does the running of various parameter look like when compared to Planck's scale M_{Pl} , whose value is around 1.22×10^{19} GeV? This is interesting point to ponder on. For this we study the running of induced G , which runs strongly in the UV and goes to zero. From observations of astrophysics and cosmology we know G_{Newton} remains constant for a large energy range. However it is usually expected that it will undergo strong running near the Planck's scale. For this reason we choose M_{Pl} in the regime where induced G witnesses a strong running *i.e.* near the point where induced G goes to zero. Once this is fixed one can plot the flow of various coupling parameters and induced masses. These are presented in figure 13 and 14.

VII. CONCLUSION

Here in this paper the idea of gravity being induced from scale-invariant theory is considered. The fundamental theory is a coupled system of scale-invariant matter and higher-derivative gravity. The lorentzian path-integral of this fundamental theory incorporates quantum fluctuations from both matter and gravity. The matter sector is taken to be simple (a scalar and a dirac fermion).

The effective action of the theory is computed in the $4 - \epsilon$ dimensional regularisation procedure. The divergent part of which gives the RG flow of the various coupling parameters of the theory. These have been computed in past also. We did it again in order to verify the past results. We agree fully with the past literature [26, 27]. We then compute the one-loop RG improved effective potential of the scalar field on the flat space-time. This gets contribution from the both the gravitational and matter degrees of freedom. This effective potential however contains an instability which comes up as an imaginary piece in the

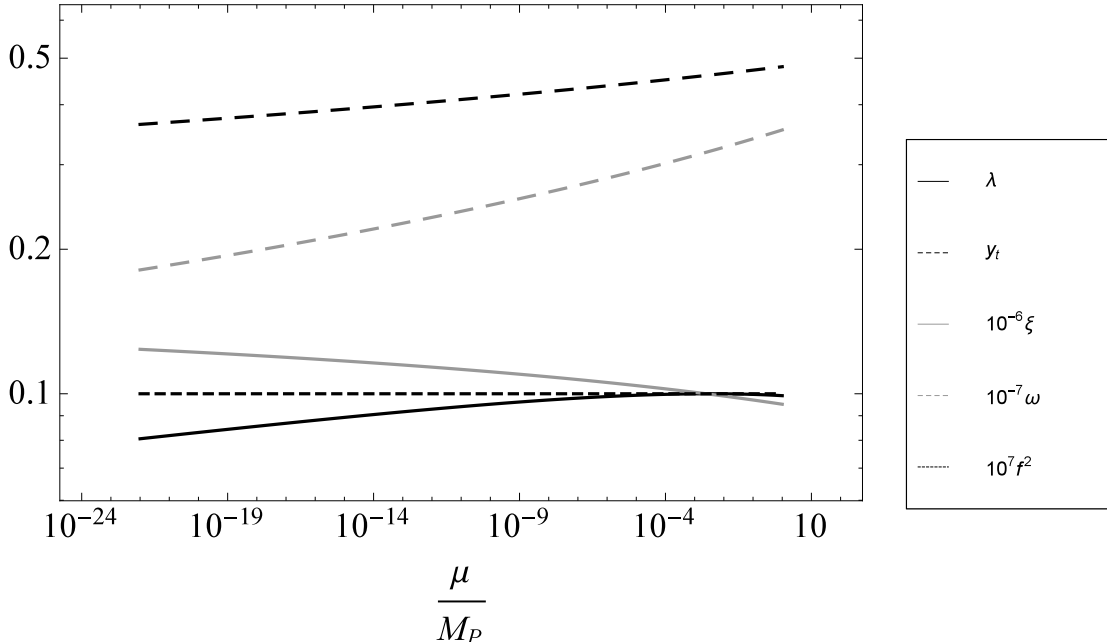


FIG. 13: The running of various dimensionless couplings. For this we took $f_*^2 = 10^{-8}$, $\lambda_* = 0.1$, $\xi_* = 10^5$. We took $\rho_* = 1.5$ and $\epsilon = 10^{-16}$, which gave $y_{t*} = 0.46$ and $\omega_* = 3.18 \times 10^6$. Here μ is the running energy scale.

effective potential. The straightforward interpretation of the appearance of an imaginary piece in the effective potential is an indication that the background (flat space-time and constant scalar background) is not stable, and will decay.

The reason for the occurrence of this instability is probed. It is found that this is purely gravitational in nature, in the sense that it arose from occurrence of tachyonic modes in the spin-2 gravitational sector and the gravitational scalar sector. These kind of tachyonic instabilities have been investigated in past [87, 88], and is a characteristic feature of gravitational theories coupled with scalar in flat space-time. At finite temperature this instability (also known as Jeans instability) results in collapse of gas of gravitons. While the occurrence of this instability is a disturbing feature of the theory and is unavoidable, it is however an IR problem and has no effect on the UV physics. In this paper we considered a different feature of theory. We investigate the issue of ghost appearing due to the presence of higher-derivative terms in the theory, which affect also the UV physics. This is done by investigating only the real part of the effective potential and ignoring the instability caused by the tachyonic modes.

The real part of effective potential develops a VeV. This breaks the scale symmetry and induces mass scale, which in turn generates Newton's constant and masses for matter fields. The propagator of the metric fluctuation field now has mass, and in the broken phase it is easy to see problematic massive tensor ghost of the theory which remains shrouded in the symmetric phase. The scalar mode (Riccion) of the metric fluctuation also picks a mass in the broken phase. The VeV has a running, which in turn induces a running in the various parameters that are generated in the broken phase. It therefore seems sensible to ask question on behaviour of massive tensor ghost under this running in the broken phase, which is the most important aim of the paper.

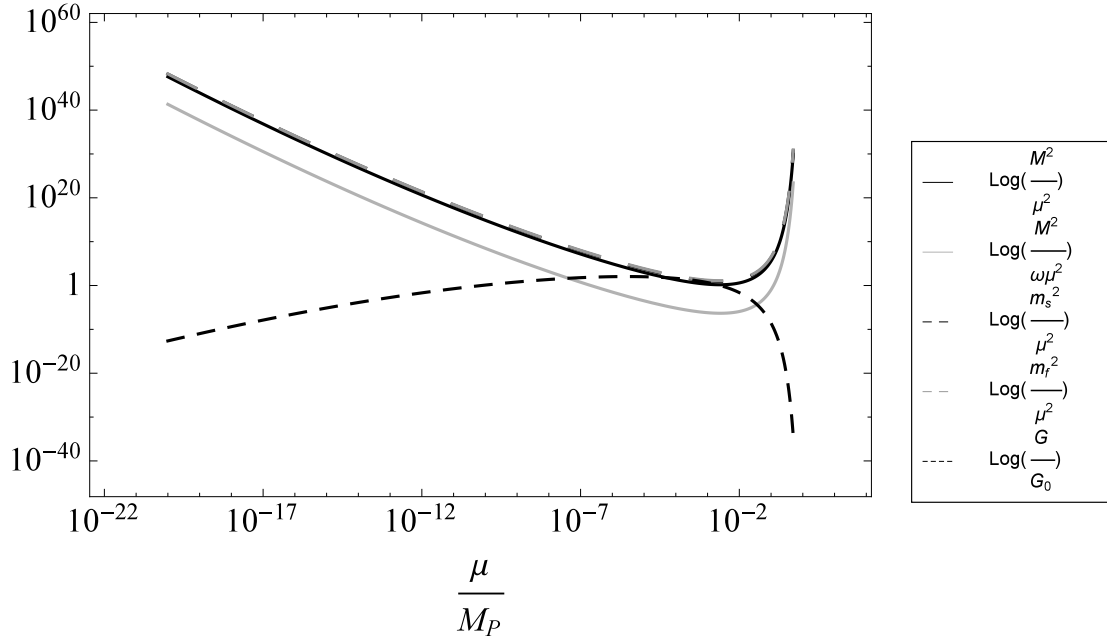


FIG. 14: The running of various induced masses and induced Newton's constant. For this we took $f_*^2 = 10^{-8}$, $\lambda_* = 0.1$, $\xi_* = 10^5$. We took $\rho_* = 1.5$ and $\epsilon = 10^{-16}$, which gave $y_{t*} = 0.46$ and $\omega_* = 3.18 \times 10^6$. Here μ is the running energy scale.

The induced running in the various parameters generated in the broken phase allows to investigate the running of M^2/μ^2 (where M is the induced mass of tensor ghost). The crucial task of the paper was to see whether there exist a domain of coupling parameters space where it is possible to make $M^2/\mu^2 > 1$ throughout the whole RG trajectory. Satisfactory arrangement of $M^2/\mu^2 > 1$ will imply that the massive tensor ghost is never physically realised and never goes on-shell. This issue is however studied numerically, as the complexity of the beta-functions and the complicated running of the induced parameters in broken phase hinders to make analytic progress.

The last part of paper is devoted to numerically studying this issue. A prescription to choose the set of initial conditions so that $M^2/\mu^2 > 1$ for whole RG trajectory is stated. This involves solving certain constraints. It is realised that the flow of M^2/μ^2 has a unique minima at a certain point along the RG trajectory. The existence of such a point was analytically proved in the context of higher-derivative gravity including Einstein-Hilbert term [5, 6], as the RG equation were simpler. In the present paper however it is not possible to achieve this analytically and numerical support was taken to get evidence for the existence of such a minima. We do see that for a large domain of parameter space such a unique minima does exist, and by requiring that $M^2/\mu^2 > 1$ at this minima implies that $M^2/\mu^2 > 1$ for whole RG trajectory. This although is not a robust analytic proof but stands as a strong evidence. We considered different set of initial conditions by varying various parameters in a systematic fashion. In each case it was see that the minima in the flow of M^2/μ^2 always exists and unitarity criterion can be met.

In this domain of coupling parameter space where $M^2/\mu^2 > 1$ for the whole RG trajectory, the behaviour of other parameters are studied. The first important thing that is noticed is the existence of a finite UV cutoff in the theory, which was also noticed in [5–8]. Even

though we do the analysis in dimensional regularisation, still a cutoff emerges dynamically from the RG equations. Beyond this point the flow cannot be continued and knowledge of higher-loop contributions are needed. In [5–8] we showed analytically that at this point the coupling ω diverges. In the present context we noticed this numerically. The behaviour of matter coupling λ has an interesting flow. It is seen to increase monotonically, but in the UV this stops and starts to decrease. This is due to yukawa coupling. The flow of yukawa coupling y_t increases monotonically, and stops when the cutoff is reached. In the case of $R\varphi^2$ coupling, the coupling starts to run only near the UV, where it is seen to go toward smaller values, hinting that there might perhaps exists a stable fixed point.

The flow of the induced Newton’s constant G is interesting. It approaches zero both in UV and IR. In UV it vanishes at finite energy scale. This was something which was also observed in [5–8], where Einstein-Hilbert was present in the bare action of the theory and was not induced. In that respect this is surprising that in the present picture of Einstein-Hilbert term being induced from scale-invariant theory, the flow of the induced gravitational coupling is qualitatively similar to the case where EH term is present in the theory to begin with. Such vanishing of induced G is although unexpected but a welcome feature. This is opposite to the widely known feature in Einstein-Hilbert gravity (without higher-derivatives) where Newton’s constant becomes very large in UV. However those results cannot be trusted as they appear in non-renormalizable theories. In the presence of higher-derivatives the situation changes in UV. Such vanishing of Newton’s constant means that in UV, gravity decouples from matter, although gravitational self-interactions continue to exist. Such a behaviour will have consequences in the early universe, and also justifies the use of flat background in the UV. This softening can also be used in addressing the Higgs naturalness problem [27].

The flow of combination $M^2/\omega\mu^2$ is however a bit different than what has been witnessed in [5–8], in the sense that the function $M^2/\omega\mu^2$ is no longer a monotonically decreasing function of RG time t . On the contrary it has a flow similar to M^2/μ^2 , having a single minima. But there is a region of RG time t over which $M^2/\omega\mu^2 < 1$. This is because of the choice of initial condition $M_*^2/\mu_*^2 = \rho_*$ we made. This will imply that there is a range of t where this scalar mode will be realised and will go on-shell, and outside this region it will remain unrealised. This can play a role in early universe to drive inflation. On the other hand the parameter ρ_* can be chosen appropriately large in order to make this scalar mode ghost (never goes on-shell), while still having unitarity.

The running of VeV also induces a running in the generated masses for the scalar and fermion. To analyse whether they are physically realised or not, we studied the behaviour of m_s^2/μ^2 and m_f^2/μ^2 respectively. It is seen that if we choose ρ_* appropriately, then it is possible to make them not physically realisable. They never go on-shell but do effect the theory gravitationally.

The RG flow equations for the dimensionless couplings are gauge independent at one-loop however at higher loop gauge dependence is expected to enter. The effective potential is gauge-dependent which is because the hessian carries gauge dependence. This gauge dependence then enters the VeV and any quantity which is related to VeV (induced Newton’s constant and induced masses). In the paper we studied the problem in Landau gauge which is a physical gauge allowing propagation of only transverse modes and suppressing longitudinal ones. However such gauge dependence is expected not to change qualitative features. This was explicitly seen in the case of pure higher-derivative gravity without matter [5, 6].

In the action appearing in the integrand for the lorentzian path-integral, the sign of coefficient of $C_{\mu\nu\rho\sigma}^2$ is taken to be negative while the sign of coefficient of R^2 is taken positive.

This is done to avoid tachyons and make the poles (in broken phase) lie on real axis, the inspiration of which comes from past study done in [5–8]. Such a choice further offers necessary convergence in the lorentzian path-integral in the feynman $+i\epsilon$ -prescription. This sign choice then implies that the coupling f^2 is no longer asymptotically free different from what is seen in path-integral defining a positive-definite euclidean theory [9, 10, 16, 30–33] (which is an entirely different theory), but instead has a Landau pole. This Landau singularity however appears way beyond the point where the RG flow of all couplings stops. Also the occurrence of Landau singularity is very possibly a one-loop effect, as at higher loops the running of f^2 gets correction thereby hinting the occurrence of fixed point [5, 6]. Moreover in this theory the dimensionless perturbative parameters f^2 , f^2/ω , $\xi\sqrt{f^2}$, $\xi\sqrt{f^2/\omega}$, λ and y_t remain small throughout the RG flow, thereby justifying the usage of perturbative approximation and we don't enter non-perturbative regimes in our analysis.

The analysis done in the paper is on a flat background. This is because any generic background has locally flat regions allowed by (strong) equivalence principle. Also when one is probing ultra-short distances, one can do the analysis on flat space-time, as the perturbative UV divergences are independent of the background. Moreover, the chances of tensor-ghost becoming physically realisable is more in UV (and nowhere else), therefore its avoidance is important in UV, which can be investigated on a flat space-time. However extrapolating flat space-time analysis in deep infrared can lead to erroneous conclusions. In performing this study cosmological constant was put to zero, and was argued that it can be maintained to be zero in a supersymmetric framework. However supersymmetry is broken in IR and this will generate cosmological constant back again. Moreover current observations also favours the existence of cosmological constant in order to drive the accelerated expansion of the universe. Therefore a proper treatment of IR physics in a field theoretic language is needed. A possible direction would be to formulate the theory on a deSitter background [92–95] (see also [96] and references therein). This will give more accurate description of the theory in the infrared.

The existence of tachyonic instability is a further indication that the chosen background of flat space-time is unstable. While this is an IR effect and an unavoidable outcome of gravitational theories coupled with scalar on flat space-time, it signals the breakdown of flat space-time as the background. It is expected that performing the study on a curved background might address these issues. For this, one would require a more accurate description of the formulation of field theory on curved background, and obtain the results in low energy limit. Alternatively one may have to incorporate non-localities appropriately to deal with IR physics [97, 98]. This is a future direction and will be considered later.

It is interesting to wonder whether the RG equations gets modified when the decoupling of massive spin-2 ghost mode occurs, in the same manner as in flat space-time non gravitational QFTs where decoupling theorem exists [99]. In flat space-time QFTs a systematic order-by-order computation leads to decoupling of heavier modes in process occurring at energies less than the mass of heavy particle. This theorem has been suitably extended to the case of matter theories on curved background [83–85], where the beta-functions gets a correction in mass-dependent scheme. For spin-2 fields the situation is a bit more involved, as incorporating mass in a diffeomorphism invariant manner is a tricky task. A possible way to achieve is by including higher-derivative terms in the action, which immediately brings in ghosts. If the ghost mass however is always above the energy scale, then ghosts get avoided due to decoupling. But this occurs in the quantum theory where RG running of the ghost mass is always above the energy scale. This implies an effective decoupling in the sense this

spin-2 ghost mode never goes on-shell and off-shell it doesn't contribute to imaginary part of amplitudes [5, 6]. But currently it is unclear how such a decoupling will modify the RG flow equations of various parameters. This is really worthy of investigations and will be considered in future works.

Acknowledgements

I would like to thank Prof. Ramesh Anishetty for several useful discussions and enlightening suggestions. I am thankful to Prof. Tianjun Li for support, encouragement and fruitful discussions. I would like to thank Nirmalya Kajuri, Nick Houston and Tuhin Mukherjee for useful discussions. I would like to thank IMSc for hosting my visit and providing hospitality, where initial stages of the work was done. I thank the referee for raising the point regarding the modification of RG equations under the decoupling of ghost modes.

Appendix A: Expansions

For the computation of the running of all couplings including wave-function renormalisation the background of flat space-time is sufficient. However for simplicity to compute the running of $R\phi^2$ coupling we employ heat kernel methods, for which we take the background to be deSitter space-time.

For the flat background we have $g_{\mu\nu} = \eta_{\mu\nu} + h_{\mu\nu}$,

$$g^{\mu\nu} = \eta^{\mu\nu} - h^{\mu\nu} + h^\mu{}_\alpha h^{\alpha\nu} + \dots \quad (\text{A1})$$

The expansion of $\sqrt{-g}$ is,

$$\sqrt{-g} = 1 + \frac{1}{2}h + \frac{1}{8}h^2 - \frac{1}{4}h_{\mu\nu}h^{\mu\nu} + \dots \quad (\text{A2})$$

The tetrads ($e^a{}_\mu$) are related with the metric by the following,

$$\eta_{ab}e^a{}_\mu e^b{}_\nu = g_{\mu\nu}. \quad (\text{A3})$$

The inverse tetrads ($e_a{}^\mu$) are similarly related with the inverse metric. Using these relations one can work out the expansion of the tetrads and inverse-tetrads in terms of the metric fluctuation field $h_{\mu\nu}$,

$$\begin{aligned} e^a{}_\mu &= \bar{e}^a{}_\rho \left(\delta^\rho{}_\mu + \frac{1}{2}h^\rho{}_\mu - \frac{1}{8}h^\rho{}_\alpha h^\alpha{}_\mu + \dots \right), \\ e_a{}^\mu &= \bar{e}_a{}^\rho \left(\delta_\rho{}^\mu - \frac{1}{2}h_\rho{}^\mu + \frac{3}{8}h_\rho{}^\alpha h_\alpha{}^\mu + \dots \right). \end{aligned} \quad (\text{A4})$$

As the determinant of tetrad e is just $\sqrt{-g}$ therefore its expansion is same as in eq. (A2).

The expansion of the christoffel connection and spin connection can be performed by first writing them in terms of metric and tetrads respectively, and then using the expansion of metric and tetrad mentioned above to obtain their expansion.

The christoffel connection is given by,

$$\Gamma_\alpha{}^\mu{}_\beta = \frac{1}{2}g^{\mu\rho}[\partial_\alpha g_{\rho\beta} + \partial_\beta g_{\rho\alpha} - \partial_\rho g_{\alpha\beta}], \quad (\text{A5})$$

Its expansion in terms of the $h_{\mu\nu}$ around the flat background is,

$$\Gamma_{\alpha}{}^{\mu}{}_{\beta} = \frac{1}{2}(\partial_{\alpha}h^{\mu}{}_{\beta} + \partial_{\beta}h^{\mu}{}_{\alpha} - \partial^{\mu}h_{\alpha\beta}) - \frac{1}{2}h^{\mu\rho}(\partial_{\alpha}h_{\rho\beta} + \partial_{\beta}h_{\rho\alpha} - \partial_{\rho}h_{\alpha\beta}) + \dots \quad (\text{A6})$$

The spin-connection $\omega_{\mu cd}$ for torsion-free space-time has a simple expression in terms of christoffel connection

$$\omega_{\mu}{}^{ad} = e^{d\nu}e^a{}_{\lambda}\Gamma_{\mu}{}^{\lambda}{}_{\nu} - e^{d\nu}\partial_{\mu}e^a{}_{\nu}. \quad (\text{A7})$$

The christoffel connection $\Gamma_{\alpha}{}^{\mu}{}_{\beta}$ can be expressed in terms of tetrads and its inverse. This when plugged in eq. (A7) gives spin-connection solely in terms of the tetrads, inverse tetrads and derivative of tetrad,

$$\omega_{\mu}{}^{ad} = \frac{1}{2} [e^{a\rho}(\partial_{\mu}e^d{}_{\rho} - \partial_{\rho}e^d{}_{\mu}) - e^{d\rho}(\partial_{\mu}e^a{}_{\rho} - \partial_{\rho}e^a{}_{\mu}) + e^b{}_{\mu}e^{a\rho}e^{d\nu}(\partial_{\nu}e_{b\rho} - \partial_{\rho}e_{b\nu})]. \quad (\text{A8})$$

By plugging the expansion of the tetrads and inverse tetrads one can obtain the expansion of the spin connection in terms of the metric fluctuation fields,

$$\omega_{\mu}{}^{ad} = (\bar{e}^{a\theta}\bar{e}^{d\tau} - \bar{e}^{a\tau}\bar{e}^{d\theta}) \left[-\partial_{\theta}h_{\tau\mu} - \frac{1}{4}h_{\theta\rho}\partial_{\mu}h_{\tau\rho} + \frac{1}{2}h_{\tau\rho}\partial_{\theta}h^{\rho}{}_{\mu} + \frac{1}{2}h_{\theta\rho}\partial_{\rho}h_{\tau\mu} + \dots \right]. \quad (\text{A9})$$

The Reimann curvature tensor is $R_{\mu\nu}{}^{\rho}{}_{\sigma} = \partial_{\mu}\Gamma_{\nu}{}^{\rho}{}_{\sigma} - \partial_{\nu}\Gamma_{\mu}{}^{\rho}{}_{\sigma} + \Gamma_{\mu}{}^{\rho}{}_{\lambda}\Gamma_{\nu}{}^{\lambda}{}_{\sigma} - \Gamma_{\nu}{}^{\rho}{}_{\lambda}\Gamma_{\mu}{}^{\lambda}{}_{\sigma}$. We are interested only in the expansion of the Ricci tensor and Ricci scalar.

$$R_{\mu\nu} = \frac{1}{2}(\partial_{\rho}\partial_{\mu}h^{\rho}{}_{\nu} + \partial_{\rho}\partial_{\nu}h^{\rho}{}_{\mu} - \square h_{\mu\nu} - \partial_{\mu}\partial_{\nu}h) + \partial_{\rho}\Gamma_{\mu}{}^{(2)\rho}{}_{\nu} - \partial_{\mu}\Gamma_{\rho}{}^{(2)\rho}{}_{\nu} + \frac{1}{4} \left[\partial^{\lambda}h(\partial_{\mu}h_{\lambda\nu} + \partial_{\nu}h_{\lambda\mu} - \partial_{\lambda}h_{\mu\nu}) - \partial_{\mu}h^{\rho\sigma}\partial_{\nu}h_{\rho\sigma} - 2\partial^{\lambda}h^{\rho}{}_{\mu}\partial_{\rho}h_{\lambda\nu} + 2\partial^{\lambda}h^{\rho}{}_{\mu}\partial_{\lambda}h_{\rho\nu} \right], \quad (\text{A10})$$

$$R = \partial_{\mu}\partial_{\nu}h^{\mu\nu} - \square h - \frac{1}{2}h^{\mu\nu}(2\partial_{\rho}\partial_{\mu}h^{\rho}{}_{\nu} - \square h_{\mu\nu} - \partial_{\mu}\partial_{\nu}h) + \eta^{\mu\nu}(\partial_{\rho}\Gamma_{\mu}{}^{(2)\rho}{}_{\nu} - \partial_{\mu}\Gamma_{\rho}{}^{(2)\rho}{}_{\nu}) + \frac{1}{4} \left[\partial^{\lambda}(2\partial^{\sigma}h_{\lambda\sigma} - \partial_{\lambda}h) + \partial^{\rho}h^{\nu\lambda}\partial_{\rho}h_{\nu\lambda} - 2\partial^{\lambda}h^{\rho\nu}\partial_{\rho}h_{\lambda\nu} \right]. \quad (\text{A11})$$

Appendix B: Projectors

The metric fluctuation field $h_{\mu\nu}$ around a general background can be decomposed into various components by doing a transverse-traceless decomposition. This is equivalent to doing decomposition of a vector into transverse and longitudinal components. For the metric fluctuation field $h_{\mu\nu}$ around a flat background, this decomposition can be written in momentum space as,

$$h_{\mu\nu} = h_{\mu\nu}^T + \iota(q_{\mu}\xi_{\nu} + q_{\nu}\xi_{\mu}) + \left(\eta_{\mu\nu} - \frac{q_{\mu}q_{\nu}}{q^2} \right) s + \frac{q_{\mu}q_{\nu}}{q^2} w. \quad (\text{B1})$$

where the various components satisfies the following constraints,

$$h_{\mu}{}^T{}^{\mu} = 0, \quad q^{\mu}h_{\mu\nu}^T = 0, \quad q^{\mu}\xi_{\mu} = 0. \quad (\text{B2})$$

Here $h_{\mu\nu}^T$ is a transverse-traceless symmetric tensor, ξ_{μ} is a transverse vector and s and w are two scalars. This decomposition can be neatly written by making use of flat space-time

projectors, which projects various components of $h_{\mu\nu}$ field into $h_{\mu\nu}^T$, ξ_μ , s and w respectively. These projectors are written in terms of the following two projectors,

$$L_{\mu\nu} = \frac{q_\mu q_\nu}{q^2} \ , \quad T_{\mu\nu} = \eta_{\mu\nu} - \frac{q_\mu q_\nu}{q^2} . \quad (\text{B3})$$

These are basically the projector for projecting out various components of a vector field. They satisfy $q^\mu T_{\mu\nu} = 0$ and $q^\mu L_{\mu\nu} = q_\nu$. Using them the projectors for the rank-2 tensor field can be constructed. These are given by,

$$(P_2)_{\mu\nu}{}^{\alpha\beta} = \frac{1}{2} [T_\mu{}^\alpha T_\nu{}^\beta + T_\mu{}^\beta T_\nu{}^\alpha] - \frac{1}{d-1} T_{\mu\nu} T^{\alpha\beta} , \quad (\text{B4})$$

$$(P_1)_{\mu\nu}{}^{\alpha\beta} = \frac{1}{8} [T_\mu{}^\alpha L_\nu{}^\beta + T_\mu{}^\beta L_\nu{}^\alpha + T_\nu{}^\alpha L_\mu{}^\beta + T_\nu{}^\beta L_\mu{}^\alpha] , \quad (\text{B5})$$

$$(P_s)_{\mu\nu}{}^{\alpha\beta} = \frac{1}{d-1} T_{\mu\nu} T^{\alpha\beta} , \quad (\text{B6})$$

$$(P_w)_{\mu\nu}{}^{\alpha\beta} = L_{\mu\nu} L^{\alpha\beta} . \quad (\text{B7})$$

The projectors for spin-2, spin-1, spin-s and spin-w form an orthogonal set. In the scalar sector there are two more projectors (which are not projectors in the strict sense), which along with spin-s and spin-w projectors form a complete set. They are given by,

$$(P_{sw})_{\mu\nu}{}^{\alpha\beta} = \frac{1}{\sqrt{d-1}} T_{\mu\nu} L^{\alpha\beta} , \quad (\text{B8})$$

$$(P_{ws})_{\mu\nu}{}^{\alpha\beta} = \frac{1}{\sqrt{d-1}} L_{\mu\nu} T^{\alpha\beta} . \quad (\text{B9})$$

The projectors in eqs. (B4, B5, B6 and B7) forms a complete set in the sense that their sum is unity.

$$(P_2)_{\mu\nu}{}^{\rho\sigma} + (P_1)_{\mu\nu}{}^{\rho\sigma} + (P_s)_{\mu\nu}{}^{\rho\sigma} + (P_w)_{\mu\nu}{}^{\rho\sigma} = \delta_{\mu\nu}^{\rho\sigma} , \quad (\text{B10})$$

where $\delta_{\mu\nu}^{\rho\sigma} = 1/2(\delta_\mu^\rho \delta_\nu^\sigma + \delta_\nu^\rho \delta_\mu^\sigma)$. Each of these projectors when act on $h_{\mu\nu}$ projects out various spin components of the tensor field.

$$\begin{aligned} (P_2)_{\mu\nu}{}^{\rho\sigma} h_{\rho\sigma} &= h_{\mu\nu}^T , & (P_1)_{\mu\nu}{}^{\rho\sigma} h_{\rho\sigma} &= \iota(q_\mu \xi_\nu + q_\nu \xi_\mu) , \\ (P_s)_{\mu\nu}{}^{\rho\sigma} h_{\rho\sigma} &= (d-1)T_{\mu\nu} s , & (P_w)_{\mu\nu}{}^{\rho\sigma} h_{\rho\sigma} &= L_{\mu\nu} w . \end{aligned} \quad (\text{B11})$$

If the projectors P_2 , P_1 , P_s and P_w are written as P_{22} , P_{11} , P_{ss} and P_{ww} respectively, then all the projectors (including P_{sw} and P_{ws}) satisfy the following algebra,

$$P_{ij} P_{mn} = \delta_{jm} P_{in} , \quad (\text{B12})$$

where i, j, m and $n = \{2, 1, s, w\}$.

Appendix C: Matter Propagator and Vertices

Here we write the propagator for matter fields and vertices of the action given in eq. (2). These are obtained by doing the second variation of the action with respect to various fields. The first line of eq. (2) gives the graviton propagator which is mentioned in eq. (17), while the second line of eq. (2) gives the propagator for the matter fields and various graviton-matter, matter-matter vertices. In the following we will be obtaining them one by one.

1. Propagators for Matter fields

Here we write the inverse propagators for the various matter fields. These are obtained by doing the second variation of the action of the theory with respect to various fields. The mixed terms in such kind of variation will be treated as interaction terms. From the second variation of the action given in eq. (19) one can pick the terms corresponding to the scalar and fermion propagator. The operator whose inverse correspond to scalar propagator is,

$$\Delta_s = -\partial^2. \quad (\text{C1})$$

In the case of fermions the relevant inverse operator is given by,

$$(\Delta_F)_{ab} = i\gamma_{ab}^\rho \partial_\rho. \quad (\text{C2})$$

2. Vertices

Here we specify the various vertices that are relevant for our one-loop computations. These can be categorised in 3 parts: (a) vertex with two internal graviton lines, (b) vertex with one internal graviton line and one internal matter line, and (c) vertex with two internal matter lines.

a. Gravity-gravity

In these vertices there are two internal graviton lines. In the following the term $V^{\mu\nu\rho\sigma}$ comes from scalar field action, while the term $U^{\mu\nu\rho\sigma}$ comes from fermion field action. The vertices are depicted in figure 15.

$$\begin{aligned} & \int d^d x h_{\mu\nu} (V^{\mu\nu\rho\sigma} + U^{\mu\nu\rho\sigma}) h_{\rho\sigma} \\ V^{\mu\nu\rho\sigma} &= \frac{1}{4} (\eta^{\mu\nu} \eta^{\rho\sigma} - \eta^{\mu\rho} \eta^{\nu\sigma} - \eta^{\mu\sigma} \eta^{\nu\rho}) \left\{ \frac{1}{2} (\partial\varphi)^2 - \frac{\lambda}{4} \varphi^4 \right\} - \frac{1}{2} \eta^{\rho\sigma} \partial^\mu \varphi \partial^\nu \varphi \\ &+ \eta^{\sigma\nu} \partial^\mu \varphi \partial^\rho \varphi - \frac{1}{2} \xi \varphi^2 \left\{ -\eta^{\nu\sigma} \partial^\mu \partial^\rho + \frac{1}{4} (\eta^{\mu\rho} \eta^{\nu\sigma} + \eta^{\mu\sigma} \eta^{\nu\rho} - 2\eta^{\mu\nu} \eta^{\rho\sigma}) \square + \eta^{\mu\nu} \partial^\rho \partial^\sigma \right\} \\ &- \xi \left\{ \varphi \partial^\mu \varphi (\eta^{\nu\rho} \partial^\sigma - 2\eta^{\rho\sigma} \partial^\nu) - \frac{1}{4} \varphi \partial^\alpha \varphi (3(\eta^{\mu\rho} \eta^{\nu\sigma} + \eta^{\mu\sigma} \eta^{\nu\rho}) - 2\eta^{\mu\nu} \eta^{\rho\sigma}) \partial_\alpha \right\} \\ &+ \frac{1}{2} \xi (\partial^\nu \varphi \partial^\beta \varphi + \varphi \partial^\nu \partial^\beta \varphi) (\eta^{\mu\rho} \delta_\beta^\sigma + \eta^{\mu\sigma} \delta_\beta^\rho), \end{aligned} \quad (\text{C3})$$

$$\begin{aligned} U^{\mu\nu\rho\sigma} &= \frac{i}{4} (\eta^{\mu\nu} \eta^{\rho\sigma} - \eta^{\mu\rho} \eta^{\nu\sigma} - \eta^{\mu\sigma} \eta^{\nu\rho}) \bar{\theta} \gamma^\tau \partial_\tau \theta - \frac{i}{2} \eta^{\mu\nu} \bar{\theta} \gamma^\rho \partial^\sigma \theta + \frac{3i}{4} \eta^{\sigma\nu} \bar{\theta} \gamma^\rho \partial^\mu \theta \\ &- \frac{i}{8} \eta^{\sigma\nu} \bar{\theta} \gamma^\tau [\gamma^\mu, \gamma^\rho] \theta \partial_\tau + \frac{i}{4} \bar{\theta} \gamma^\rho [\gamma^\mu, \gamma^\sigma] \theta \partial^\nu - \frac{i}{4} \eta^{\nu\sigma} \partial_\alpha \{ \bar{\theta} \gamma^\rho [\gamma^\alpha, \gamma^\mu] \theta \} - \frac{i}{4} \eta^{\mu\nu} \bar{\theta} \gamma^\rho [\gamma^\alpha, \gamma^\sigma] \theta \partial_\alpha \\ &- \frac{1}{4} y_t \varphi (\eta^{\mu\nu} \eta^{\rho\sigma} - \eta^{\mu\rho} \eta^{\nu\sigma} - \eta^{\mu\sigma} \eta^{\nu\rho}) \bar{\theta} \theta. \end{aligned} \quad (\text{C4})$$



FIG. 15: Various vertices containing two internal graviton lines. Here the dashed line is scalar, solid line with arrow is fermion, while double line depicts graviton. The lines ending with circle containing cross are external legs.

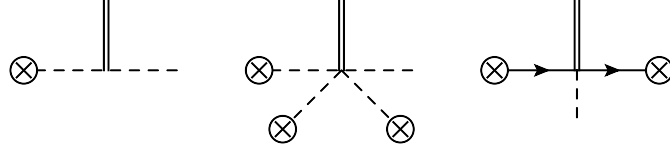


FIG. 16: Various vertices containing one internal graviton line and one internal scalar leg. Here the dashed line is scalar, solid line with arrow is fermion, while double line depicts graviton. The lines ending with circle containing cross are external legs.

b. Gravity-scalar

Here we write the vertex which has one internal graviton line and one internal scalar line. This vertex gets contribution from both scalar and fermion field actions. These vertices are depicted in figure 16.

$$\int d^d x [h_{\rho\sigma}(V_{h\phi})^{\rho\sigma}\chi + \chi(V_{\phi h})^{\mu\nu}h_{\mu\nu}]$$

$$(V_{h\phi})_{\rho\sigma} = -\frac{\lambda}{2}\varphi^2\eta_{\rho\sigma}\varphi + \frac{1}{2}\eta_{\rho\sigma}\partial_\alpha\varphi\partial^\alpha - \partial_\rho\varphi\partial_\sigma - \xi\{\partial_\rho\partial_\sigma\varphi + \partial_\rho\varphi\partial_\sigma + \partial_\sigma\varphi\partial_\rho + \varphi\partial_\rho\partial_\sigma\}$$

$$+\xi\eta_{\rho\sigma}(\square\varphi + 2\partial_\alpha\varphi\partial^\alpha + \varphi\square) - \frac{1}{2}\eta_{\rho\sigma}y_t\bar{\theta}\theta, \quad (\text{C5})$$

$$(V_{\phi h})_{\mu\nu} = -\frac{\lambda}{2}\lambda\varphi^2\eta_{\mu\nu}\varphi - \frac{1}{2}\eta_{\mu\nu}\partial_\beta\varphi\partial^\beta - \frac{1}{2}\eta_{\mu\nu}\square\varphi + \partial_\mu\varphi\partial_\nu + \partial_\mu\partial_\nu\varphi$$

$$-\xi\varphi(\partial_\mu\partial_\nu - \eta_{\mu\nu}\square) - \frac{1}{2}\eta_{\mu\nu}y_t\bar{\theta}\theta. \quad (\text{C6})$$

c. Gravity-fermion

Here we write the vertex that contain one internal graviton line and one internal fermion line. These vertex comes only from the fermion field action. These vertices are depicted in figure 17.

$$\int d^d x [\bar{\eta}_d(V_{\bar{\psi}h})^{\rho\sigma}h_{\rho\sigma} + h_{\mu\nu}(V_{h\bar{\psi}}^T)^{\mu\nu}\bar{\eta}_c^T],$$

$$(V_{\bar{\psi}h})_{d\rho\sigma} = \frac{i}{2}(\eta_{\rho\sigma}\gamma_{de}^\tau\partial_\tau\theta_e - (\gamma_\rho)_{de}\partial_\nu\theta_e) - \frac{i}{4}(\gamma_\rho[\gamma^\alpha, \gamma_\sigma])_{de}\theta_e\partial_\alpha - \frac{y_t}{2}\varphi\eta_{\rho\sigma}\theta_d, \quad (\text{C7})$$

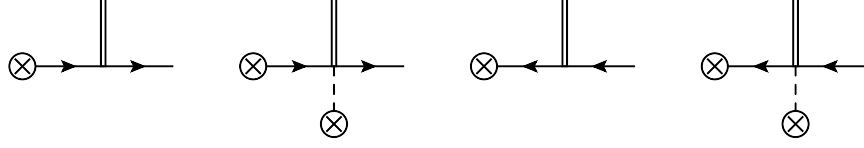


FIG. 17: Various vertices containing one internal graviton line and one internal fermion leg. Here the dashed line is scalar, solid line with arrow is fermion, while double line depicts graviton. The lines ending with circle containing cross are external legs.

$$\begin{aligned}
(V_{h\bar{\psi}}^T)^{\mu\nu} &= -\frac{i}{2} \{ \eta^{\mu\nu} \partial_\tau \theta_e (\gamma^{T\tau})_{ec} - (\partial^\nu \theta_e^T) \gamma_{ec}^{T\mu} \} - \frac{i}{4} (\partial_\alpha \theta_e^T) \{ [\gamma^{\mu T}, \gamma^{\alpha T}] \gamma^{\nu T} \}_{ec} \\
&- \frac{i}{4} (\theta_e^T) \{ [\gamma^{\mu T}, \gamma^{\alpha T}] \gamma^{\nu T} \}_{ec} \partial_\alpha + \frac{1}{4} \eta^{\mu\nu} y_t \varphi \theta_c^T.
\end{aligned} \tag{C8}$$

$$\begin{aligned}
&\int d^d x [h_{\mu\nu} (V_{h\psi})^{\mu\nu}_a \eta_a + \eta_a^T (V_{\psi h}^T)^{\rho\sigma} h_{\rho\sigma}], \\
(V_{h\psi})^{\mu\nu}_c &= \frac{i}{2} \{ \eta^{\mu\nu} \bar{\theta}_e \gamma_{ec}^T \partial_\tau - \bar{\theta}_e \gamma_{ec}^\nu \partial^\mu \} + \frac{i}{4} \{ (\partial_\alpha \bar{\theta}_e) (\gamma^\nu [\gamma^\alpha, \gamma^\mu])_{ec} + \bar{\theta}_e (\gamma^\nu [\gamma^\alpha, \gamma^\mu])_{ec} \partial_\alpha \} \\
&- \frac{y_t}{4} \eta^{\mu\nu} \varphi \bar{\theta}_c,
\end{aligned} \tag{C9}$$

$$\begin{aligned}
(V_{\psi h}^T)^{\rho\sigma}_b &= \frac{i}{2} \{ \eta^{\rho\sigma} \gamma_{be}^{T\tau} (\bar{\theta}_e^T \partial_\tau + \partial_\tau \bar{\theta}_e^T) - \gamma_{be}^{T\sigma} (\bar{\theta}_e^T \partial^\rho + \partial^\rho \bar{\theta}_e^T) \} + \frac{i}{4} ([\gamma^{T\rho}, \gamma^{T\alpha}] \gamma^{T\sigma})_{be} \bar{\theta}_e^T \partial_\alpha \\
&+ \frac{y_t}{2} \eta^{\rho\sigma} \bar{\theta}_b^T \varphi.
\end{aligned} \tag{C10}$$

d. Matter-matter

Here we write the vertices which has two internal matter lines. These will be either both scalar lines, one scalar and one fermion line or both fermion lines. These vertices are depicted in figure 18.

$$\begin{aligned}
&\int d^d x [-\chi (V_s) \chi + \bar{\eta}_a (V_{\bar{\psi}\psi})^{ab} \eta_b + \eta_a^T (V_{\bar{\psi}\psi}^T)^{ab} \bar{\eta}_b^T \\
&+ \bar{\eta}_a (V_{\bar{\psi}\phi})^a \chi + \chi (V_{\bar{\psi}\phi}^T)^b \bar{\eta}_b^T + \chi (V_{\phi\psi})^b \eta_b + \eta_a^T (V_{\phi\psi}^T)^a \chi] \\
V_s &= 3\lambda\varphi^2,
\end{aligned} \tag{C11}$$

$$(V_{\bar{\psi}\psi})^{ab} = -y_t \varphi \delta^{ab}, \quad (V_{\bar{\psi}\psi}^T)^{ab} = y_t \varphi \delta^{ab}, \tag{C12}$$

$$(V_{\bar{\psi}\phi})^a = -y_t \theta^a, \quad (V_{\bar{\psi}\phi}^T)^a = y_t \theta^{Ta} \tag{C13}$$

$$(V_{\phi\psi})^b = -y_t \bar{\theta}^b, \quad (V_{\phi\psi}^T)^b = y_t \bar{\theta}^{Tb}. \tag{C14}$$

Appendix D: Cubic Equation

Here we will consider the roots of generic cubic equation with real coefficients. Such an equation emerges in section. III while computing the contribution to the scalar effective

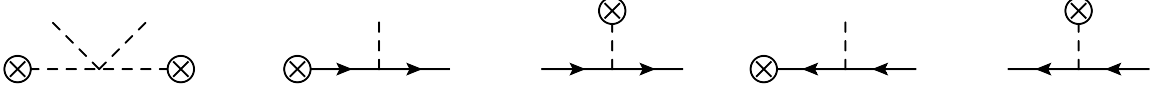


FIG. 18: Various vertices containing two internal matter legs (scalar-scalar, scalar-fermion, fermion-fermion). Here the dashed line is scalar while solid line with arrow is fermion. The lines ending with circle containing cross are external legs.

potential from the scalar sector of theory. In order to compute the contribution of the scalar to the effective potential we need analyse a cubic equation in $-\square$ operator written in eq. (62). Here in this section we will consider a generic cubic equation of the form

$$az^3 + bz^2 + cz + d = 0. \quad (\text{D1})$$

By a change of variable $z = u - b/3a$, this equation becomes a depressed cubic

$$u^3 - \frac{\Delta_0}{3a^2}u + \frac{\Delta_1}{27a^3} = 0, \quad (\text{D2})$$

$$\Delta_0 = b^2 - 3ac, \quad \Delta_1 = 2b^3 - 9abc + 27da^2. \quad (\text{D3})$$

By choosing $u = v + \Delta_0/9a^2v$, this equation can be converted in to a quadratic equation in v^3

$$v^6 + \frac{\Delta_1}{27a^3}v^3 + \frac{\Delta_0^3}{729a^6} = 0. \quad (\text{D4})$$

This quadratic equation can be solved by known algebraic methods and has two roots. The nature of roots can be determined by the sign of the discriminant of this quadratic equation.

$$-27a^2\Delta = \Delta_1^2 - 4\Delta_0^3, \quad (\text{D5})$$

where Δ was also defined in eq. (63). The two roots of the quadratic equation will be given by,

$$v^3 = \frac{-\Delta_1 \pm \sqrt{\Delta_1^2 - 4\Delta_0^3}}{54a^3} = \frac{1}{27a^3}l_{1,2}^3. \quad (\text{D6})$$

This can be solved easily by taking cube-root. Here there will be three roots for v . Corresponding to each cube-root we have a root for the eq. (D1), which is obtained by plugging v back in to u and z . The three roots will be given in terms of l_1 and l_2

$$\begin{aligned} z_1 &= \frac{1}{3a}(-b + l_1 + l_2), \\ z_2 &= \frac{1}{3a}(-b + e^{2\pi i/3}l_1 + e^{4\pi i/3}l_2), \\ z_3 &= \frac{1}{3a}(-b + e^{4\pi i/3}l_1 + e^{2\pi i/3}l_2). \end{aligned} \quad (\text{D7})$$

In the case when the discriminant $\Delta_1^2 - 4\Delta_0^3 > 0$, we have one real root and a complex conjugate pair. In this case we can write the exponentials in terms of sine and cosine functions. One can then write the real and imaginary part of these roots. This complex conjugate pair can be written in polar form also with

$$\begin{aligned} r &= \frac{1}{3a} \sqrt{b^2 + l_1^2 + l_2^2 - 2 \cos\left(\frac{2\pi}{3}\right)(bl_1 + bl_2 + l_1l_2)}, \\ \tan \theta &= \frac{\sin(2\pi/3)(l_1 - l_2)}{-b + \cos(2\pi/3)(l_1 + l_2)}, \quad \text{with } -\frac{\pi}{2} \leq \theta \leq \frac{\pi}{2}. \end{aligned} \quad (\text{D8})$$

In the case when the discriminant $\Delta_1^2 - 4\Delta_0^3 < 0$, we have a complex conjugate pair of roots for v^3 , meaning l_1 and l_2 will be complex conjugate. This will imply that expression for z_1 , z_2 and z_3 are real. However now θ appearing in eq. (D8) will be imaginary.

-
- [1] K. S. Stelle, “Classical Gravity with Higher Derivatives,” *Gen. Rel. Grav.* **9**, 353 (1978). doi:10.1007/BF00760427
 - [2] K. S. Stelle, “Renormalization of Higher Derivative Quantum Gravity,” *Phys. Rev. D* **16**, 953 (1977). doi:10.1103/PhysRevD.16.953.
 - [3] A. Salam and J. A. Strathdee, “Remarks on High-energy Stability and Renormalizability of Gravity Theory,” *Phys. Rev. D* **18**, 4480 (1978). doi:10.1103/PhysRevD.18.4480
 - [4] J. Julve and M. Tonin, “Quantum Gravity with Higher Derivative Terms,” *Nuovo Cim. B* **46**, 137 (1978). doi:10.1007/BF02748637
 - [5] G. Narain and R. Anishetty, “Short Distance Freedom of Quantum Gravity,” *Phys. Lett. B* **711**, 128 (2012) doi:10.1016/j.physletb.2012.03.070 [arXiv:1109.3981 [hep-th]].
 - [6] G. Narain and R. Anishetty, “Unitary and Renormalizable Theory of Higher Derivative Gravity,” *J. Phys. Conf. Ser.* **405**, 012024 (2012) doi:10.1088/1742-6596/405/1/012024 [arXiv:1210.0513 [hep-th]].
 - [7] G. Narain and R. Anishetty, “Charge Renormalization due to Graviton Loops,” *JHEP* **1307**, 106 (2013) doi:10.1007/JHEP07(2013)106 [arXiv:1211.5040 [hep-th]].
 - [8] G. Narain and R. Anishetty, “Running Couplings in Quantum Theory of Gravity Coupled with Gauge Fields,” *JHEP* **1310**, 203 (2013) doi:10.1007/JHEP10(2013)203 [arXiv:1309.0473 [hep-th]].
 - [9] E. S. Fradkin and A. A. Tseytlin, “Renormalizable Asymptotically Free Quantum Theory of Gravity,” *Phys. Lett.* **104B**, 377 (1981). doi:10.1016/0370-2693(81)90702-4
 - [10] E. S. Fradkin and A. A. Tseytlin, “Renormalizable asymptotically free quantum theory of gravity,” *Nucl. Phys. B* **201** (1982) 469. doi:10.1016/0550-3213(82)90444-8
 - [11] L. Alvarez-Gaume, A. Kehagias, C. Kounnas, D. Lust and A. Riotto, “Aspects of Quadratic Gravity,” *Fortsch. Phys.* **64**, no. 2-3, 176 (2016) doi:10.1002/prop.201500100 [arXiv:1505.07657 [hep-th]].
 - [12] D. M. Capper and M. J. Duff, “Trace anomalies in dimensional regularization,” *Nuovo Cim. A* **23**, 173 (1974). doi:10.1007/BF02748300
 - [13] S. Deser, M. J. Duff and C. J. Isham, “Nonlocal Conformal Anomalies,” *Nucl. Phys. B* **111** (1976) 45. doi:10.1016/0550-3213(76)90480-6
 - [14] M. J. Duff, “Observations on Conformal Anomalies,” *Nucl. Phys. B* **125** (1977) 334. doi:10.1016/0550-3213(77)90410-2
 - [15] N. H. Barth and S. M. Christensen, “Quantizing Fourth Order Gravity Theories. 1. The Functional Integral,” *Phys. Rev. D* **28**, 1876 (1983). doi:10.1103/PhysRevD.28.1876
 - [16] I. G. Avramidi and A. O. Barvinsky, “Asymptotic Freedom In Higher Derivative Quantum Gravity,” *Phys. Lett.* **159B**, 269 (1985). doi:10.1016/0370-2693(85)90248-5
 - [17] I. L. Buchbinder, O. K. Kalashnikov, I. L. Shapiro, V. B. Vologodsky and J. J. Wolfengaut, “The Stability of Asymptotic Freedom in Grand Unified Models Coupled to R^2 Gravity,” *Phys. Lett. B* **216**, 127 (1989). doi:10.1016/0370-2693(89)91381-6
 - [18] I. L. Shapiro, “Asymptotic Behavior of Effective Yukawa Coupling Constants in Quantum R^2 Gravity With Matter,” *Class. Quant. Grav.* **6**, 1197 (1989). doi:10.1088/0264-9381/6/8/019

- [19] S. D. Odintsov, “The Parametrization Invariant and Gauge Invariant Effective Actions in Quantum Field Theory,” *Fortsch. Phys.* **38**, 371 (1990).
- [20] E. Elizalde, S. D. Odintsov and A. Romeo, “Improved effective potential in curved space-time and quantum matter, higher derivative gravity theory,” *Phys. Rev. D* **51**, 1680 (1995) doi:10.1103/PhysRevD.51.1680 [hep-th/9410113].
- [21] E. Elizalde, C. O. Lousto, S. D. Odintsov and A. Romeo, “GUTs in curved space-time: Running gravitational constants, Newtonian potential and the quantum corrected gravitational equations,” *Phys. Rev. D* **52**, 2202 (1995) doi:10.1103/PhysRevD.52.2202 [hep-th/9504014].
- [22] E. Elizalde, S. D. Odintsov and A. Romeo, “Manifestations of quantum gravity in scalar QED phenomena,” *Phys. Rev. D* **51**, 4250 (1995) doi:10.1103/PhysRevD.51.4250 [hep-th/9410028].
- [23] I. L. Buchbinder, S. D. Odintsov and I. L. Shapiro, “Effective action in quantum gravity,” Bristol, UK: IOP (1992) 413 p
- [24] G. de Berredo-Peixoto and I. L. Shapiro, “Conformal quantum gravity with the Gauss-Bonnet term,” *Phys. Rev. D* **70**, 044024 (2004) doi:10.1103/PhysRevD.70.044024 [hep-th/0307030].
- [25] G. de Berredo-Peixoto and I. L. Shapiro, “Higher derivative quantum gravity with Gauss-Bonnet term,” *Phys. Rev. D* **71**, 064005 (2005) doi:10.1103/PhysRevD.71.064005 [hep-th/0412249].
- [26] A. Salvio and A. Strumia, “Agravity,” *JHEP* **1406** (2014) 080 doi:10.1007/JHEP06(2014)080 [arXiv:1403.4226 [hep-ph]].
- [27] A. Salvio, “Solving the Standard Model Problems in Softened Gravity,” *Phys. Rev. D* **94**, no. 9, 096007 (2016) doi:10.1103/PhysRevD.94.096007 [arXiv:1608.01194 [hep-ph]].
- [28] K. Kannike, G. Htsi, L. Pizza, A. Racioppi, M. Raidal, A. Salvio and A. Strumia, “Dynamically Induced Planck Scale and Inflation,” *JHEP* **1505**, 065 (2015) doi:10.1007/JHEP05(2015)065 [arXiv:1502.01334 [astro-ph.CO]].
- [29] A. Salvio and A. Strumia, “Quantum mechanics of 4-derivative theories,” *Eur. Phys. J. C* **76** (2016) no.4, 227 doi:10.1140/epjc/s10052-016-4079-8 [arXiv:1512.01237 [hep-th]].
- [30] M. B. Einhorn and D. R. T. Jones, “Naturalness and Dimensional Transmutation in Classically Scale-Invariant Gravity,” *JHEP* **1503**, 047 (2015) doi:10.1007/JHEP03(2015)047 [arXiv:1410.8513 [hep-th]].
- [31] T. Jones and M. Einhorn, “Quantum Gravity and Dimensional Transmutation,” *PoS PLANCK* **2015**, 061 (2015).
- [32] M. B. Einhorn and D. R. T. Jones, “Induced Gravity I: Real Scalar Field,” *JHEP* **1601**, 019 (2016) doi:10.1007/JHEP01(2016)019 [arXiv:1511.01481 [hep-th]].
- [33] M. B. Einhorn and D. R. T. Jones, “Induced Gravity II: Grand Unification,” *JHEP* **1605**, 185 (2016) doi:10.1007/JHEP05(2016)185 [arXiv:1602.06290 [hep-th]].
- [34] B. Holdom and J. Ren, “QCD analogy for quantum gravity,” *Phys. Rev. D* **93**, no. 12, 124030 (2016) doi:10.1103/PhysRevD.93.124030 [arXiv:1512.05305 [hep-th]].
- [35] B. Holdom and J. Ren, “Quadratic gravity: from weak to strong,” *Int. J. Mod. Phys. D* **25**, no. 12, 1643004 (2016) doi:10.1142/S0218271816430045 [arXiv:1605.05006 [hep-th]].
- [36] Y. B. Zeldovich, “Cosmological Constant and Elementary Particles,” *JETP Lett.* **6**, 316 (1967) [*Pisma Zh. Eksp. Teor. Fiz.* **6**, 883 (1967)].
- [37] A. D. Sakharov, “Vacuum quantum fluctuations in curved space and the theory of gravitation,” *Sov. Phys. Dokl.* **12**, 1040 (1968) [*Dokl. Akad. Nauk Ser. Fiz.* **177**, 70 (1967)] [*Sov. Phys. Usp.* **34**, 394 (1991)] [*Gen. Rel. Grav.* **32**, 365 (2000)].
- [38] Y. Fujii, “Scalar-tensor theory of gravitation and spontaneous breakdown of scale invariance,” *Phys. Rev. D* **9** (1974) 874. doi:10.1103/PhysRevD.9.874

- [39] E. M. Chudnovsky, “The Spontaneous Conformal Symmetry Breaking and Higgs Model,” *Theor. Math. Phys.* **35**, 538 (1978) [*Teor. Mat. Fiz.* **35**, 398 (1978)]. doi:10.1007/BF01036453
- [40] A. Zee, “A Broken Symmetric Theory of Gravity,” *Phys. Rev. Lett.* **42** (1979) 417. doi:10.1103/PhysRevLett.42.417
- [41] S. L. Adler, “A Formula for the Induced Gravitational Constant,” *Phys. Lett. B* **95**, 241 (1980). doi:10.1016/0370-2693(80)90478-5
- [42] S. L. Adler, “Order R Vacuum Action Functional in Scalar Free Unified Theories with Spontaneous Scale Breaking,” *Phys. Rev. Lett.* **44** (1980) 1567. doi:10.1103/PhysRevLett.44.1567
- [43] S. L. Adler, “Induced gravitation,” *AIP Conf. Proc.* **68** (1980) 915. doi:10.1063/1.2948651
- [44] A. Zee, “Spontaneously Generated Gravity,” *Phys. Rev. D* **23**, 858 (1981). doi:10.1103/PhysRevD.23.858
- [45] S. L. Adler, “Einstein Gravity as a Symmetry Breaking Effect in Quantum Field Theory,” *Rev. Mod. Phys.* **54** (1982) 729 Erratum: [*Rev. Mod. Phys.* **55** (1983) 837]. doi:10.1103/RevModPhys.54.729
- [46] S. R. Coleman and E. J. Weinberg, “Radiative Corrections as the Origin of Spontaneous Symmetry Breaking,” *Phys. Rev. D* **7**, 1888 (1973). doi:10.1103/PhysRevD.7.1888
- [47] R. I. Nepomechie, “Einstein Gravity as the Low-energy Effective Theory of Weyl Gravity,” *Phys. Lett.* **136B**, 33 (1984). doi:10.1016/0370-2693(84)92050-1
- [48] A. Zee, “Einstein Gravity Emerging From Quantum Weyl Gravity,” *Annals Phys.* **151**, 431 (1983). doi:10.1016/0003-4916(83)90286-5
- [49] I. L. Buchbinder, “Mechanism For Induction Of Einstein Gravitation,” *Sov. Phys. J.* **29**, 220 (1986). doi:10.1007/BF00891883
- [50] I. L. Shapiro and G. Cognola, “Interaction of low-energy induced gravity with quantized matter and phase transition induced to curvature,” *Phys. Rev. D* **51**, 2775 (1995) doi:10.1103/PhysRevD.51.2775 [hep-th/9406027].
- [51] R. Floreanini and R. Percacci, “Average effective potential for the conformal factor,” *Nucl. Phys. B* **436**, 141 (1995) doi:10.1016/0550-3213(95)00479-C [hep-th/9305172].
- [52] R. Floreanini and R. Percacci, “The Renormalization group flow of the Dilaton potential,” *Phys. Rev. D* **52**, 896 (1995) doi:10.1103/PhysRevD.52.896 [hep-th/9412181].
- [53] F. Cooper and G. Venturi, “Cosmology and Broken Scale Invariance,” *Phys. Rev. D* **24**, 3338 (1981). doi:10.1103/PhysRevD.24.3338
- [54] F. Finelli, A. Tronconi and G. Venturi, “Dark Energy, Induced Gravity and Broken Scale Invariance,” *Phys. Lett. B* **659**, 466 (2008) doi:10.1016/j.physletb.2007.11.053 [arXiv:0710.2741 [astro-ph]].
- [55] C. Ford, D. R. T. Jones, P. W. Stephenson and M. B. Einhorn, “The Effective potential and the renormalization group,” *Nucl. Phys. B* **395**, 17 (1993) doi:10.1016/0550-3213(93)90206-5 [hep-lat/9210033].
- [56] R. Percacci, “Asymptotic Safety,” In *Oriti, D. (ed.): Approaches to quantum gravity* 111-128 [arXiv:0709.3851 [hep-th]].
- [57] A. Codello and R. Percacci, “Fixed points of higher derivative gravity,” *Phys. Rev. Lett.* **97**, 221301 (2006) doi:10.1103/PhysRevLett.97.221301 [hep-th/0607128].
- [58] A. Codello, R. Percacci and C. Rahmede, “Investigating the Ultraviolet Properties of Gravity with a Wilsonian Renormalization Group Equation,” *Annals Phys.* **324**, 414 (2009) doi:10.1016/j.aop.2008.08.008 [arXiv:0805.2909 [hep-th]].
- [59] K. Groh, S. Rechenberger, F. Saueressig and O. Zanusso, “Higher Derivative Gravity from the Universal Renormalization Group Machine,” *PoS EPS -HEP2011*, 124 (2011)

- [arXiv:1111.1743 [hep-th]].
- [60] N. Ohta and R. Percacci, “Higher Derivative Gravity and Asymptotic Safety in Diverse Dimensions,” *Class. Quant. Grav.* **31** (2014) 015024 doi:10.1088/0264-9381/31/1/015024 [arXiv:1308.3398 [hep-th]].
- [61] N. Ohta and R. Percacci, “Ultraviolet Fixed Points in Conformal Gravity and General Quadratic Theories,” *Class. Quant. Grav.* **33**, 035001 (2016) doi:10.1088/0264-9381/33/3/035001 [arXiv:1506.05526 [hep-th]].
- [62] N. Ohta, R. Percacci and A. D. Pereira, “Gauges and functional measures in quantum gravity II: Higher derivative gravity,” arXiv:1610.07991 [hep-th].
- [63] M. R. Niedermaier, “Gravitational Fixed Points from Perturbation Theory,” *Phys. Rev. Lett.* **103**, 101303 (2009). doi:10.1103/PhysRevLett.103.101303
- [64] D. Benedetti, P. F. Machado and F. Saueressig, “Asymptotic safety in higher-derivative gravity,” *Mod. Phys. Lett. A* **24**, 2233 (2009) doi:10.1142/S0217732309031521 [arXiv:0901.2984 [hep-th]].
- [65] D. Benedetti, P. F. Machado and F. Saueressig, “Taming perturbative divergences in asymptotically safe gravity,” *Nucl. Phys. B* **824**, 168 (2010) doi:10.1016/j.nuclphysb.2009.08.023 [arXiv:0902.4630 [hep-th]].
- [66] L. Modesto, “Super-renormalizable Quantum Gravity,” *Phys. Rev. D* **86**, 044005 (2012) doi:10.1103/PhysRevD.86.044005 [arXiv:1107.2403 [hep-th]].
- [67] T. Biswas, E. Gerwick, T. Koivisto and A. Mazumdar, “Towards singularity and ghost free theories of gravity,” *Phys. Rev. Lett.* **108**, 031101 (2012) doi:10.1103/PhysRevLett.108.031101 [arXiv:1110.5249 [gr-qc]].
- [68] L. Modesto and L. Rachwal, “Super-renormalizable and finite gravitational theories,” *Nucl. Phys. B* **889**, 228 (2014) doi:10.1016/j.nuclphysb.2014.10.015 [arXiv:1407.8036 [hep-th]].
- [69] E. T. Tomboulis, “Renormalization and unitarity in higher derivative and nonlocal gravity theories,” *Mod. Phys. Lett. A* **30**, no. 03n04, 1540005 (2015). doi:10.1142/S0217732315400052
- [70] B. S. DeWitt, “A Gauge Invariant Effective Action,” In *Oxford 1980, Proceedings, Quantum Gravity 2*, 449-487 and Calif. Univ. Santa Barbara - NSF-ITP-80-031 (80,REC.AUG.) 54 P. (009106) (SEE CONFERENCE INDEX)
- [71] L. F. Abbott, “The Background Field Method Beyond One Loop,” *Nucl. Phys. B* **185**, 189 (1981).
- [72] L. D. Faddeev and V. N. Popov, “Feynman Diagrams for the Yang-Mills Field,” *Phys. Lett. B* **25**, 29 (1967).
- [73] R. E. Kallosh, “Modified Feynman Rules in Supergravity,” *Nucl. Phys. B* **141**, 141 (1978).
- [74] N. K. Nielsen, “Ghost Counting In Supergravity,” *Nucl. Phys. B* **140**, 499 (1978).
- [75] B. S. DeWitt, “Dynamical theory of groups and fields,” *Conf. Proc. C* **630701**, 585 (1964) [Les Houches Lect. Notes **13**, 585 (1964)].
- [76] D. V. Vassilevich, “Heat kernel expansion: User’s manual,” *Phys. Rept.* **388**, 279 (2003) doi:10.1016/j.physrep.2003.09.002 [hep-th/0306138].
- [77] S. Yajima, “Evaluation of Heat Kernel in Curved Space,” *Class. Quant. Grav.* **5**, L207 (1988). doi:10.1088/0264-9381/5/12/003
- [78] I. G. Avramidi, “Heat kernel and quantum gravity,” *Lect. Notes Phys. M* **64**, 1 (2000). doi:10.1007/3-540-46523-5
- [79] J. M. Martín-García, “xAct: Efficient Tensor Computer Algebra” [<http://www.xact.es>]
- [80] T. Nutma, “xTras: A field-theory inspired xAct package for mathematica”, *Comput. Phys. Commun.* **185**, 1719 (2014) [cs.SC/1308.3493]

- [81] R. Mertig, M. Bohm and A. Denner, “FEYN CALC: Computer algebraic calculation of Feynman amplitudes,” *Comput. Phys. Commun.* **64**, 345 (1991). doi:10.1016/0010-4655(91)90130-D
- [82] E. Elizalde, S. D. Odintsov and A. Romeo, “Renormalization group properties of higher derivative quantum gravity with matter in (4-epsilon)-dimensions,” *Nucl. Phys. B* **462**, 315 (1996) doi:10.1016/0550-3213(95)00674-5 [hep-th/9502131].
- [83] E. V. Gorbar and I. L. Shapiro, “Renormalization group and decoupling in curved space,” *JHEP* **0302**, 021 (2003) doi:10.1088/1126-6708/2003/02/021 [hep-ph/0210388].
- [84] E. V. Gorbar and I. L. Shapiro, “Renormalization group and decoupling in curved space. 2. The Standard model and beyond,” *JHEP* **0306**, 004 (2003) doi:10.1088/1126-6708/2003/06/004 [hep-ph/0303124].
- [85] E. V. Gorbar and I. L. Shapiro, “Renormalization group and decoupling in curved space. 3. The Case of spontaneous symmetry breaking,” *JHEP* **0402**, 060 (2004) doi:10.1088/1126-6708/2004/02/060 [hep-ph/0311190].
- [86] Y. Yoon and Y. Yoon, “Asymptotic conformal invariance of SU(2) and standard models in curved space-time,” *Int. J. Mod. Phys. A* **12**, 2903 (1997) doi:10.1142/S0217751X97001602 [hep-th/9612001].
- [87] D. J. Gross, M. J. Perry and L. G. Yaffe, “Instability of Flat Space at Finite Temperature,” *Phys. Rev. D* **25**, 330 (1982). doi:10.1103/PhysRevD.25.330
- [88] S. Bhattacharjee and P. Majumdar, “Gravitational Coleman-Weinberg potential and its finite temperature counterpart,” *Nucl. Phys. B* **885**, 481 (2014) doi:10.1016/j.nuclphysb.2014.05.031 [arXiv:1210.0497 [hep-th]].
- [89] S. C. Lee and P. van Nieuwenhuizen, “Counting of States in Higher Derivative Field Theories,” *Phys. Rev. D* **26** (1982) 934. doi:10.1103/PhysRevD.26.934
- [90] R. J. Riegert, “The Particle Content Of Linearized Conformal Gravity,” *Phys. Lett. A* **105**, 110 (1984). doi:10.1016/0375-9601(84)90648-0
- [91] V. Branchina and E. Messina, “Stability, Higgs Boson Mass and New Physics,” *Phys. Rev. Lett.* **111**, 241801 (2013) doi:10.1103/PhysRevLett.111.241801 [arXiv:1307.5193 [hep-ph]].
- [92] M. B. Einhorn and F. Larsen, “Interacting quantum field theory in de Sitter vacua,” *Phys. Rev. D* **67**, 024001 (2003) doi:10.1103/PhysRevD.67.024001 [hep-th/0209159].
- [93] A. M. Polyakov, “De Sitter space and eternity,” *Nucl. Phys. B* **797**, 199 (2008) doi:10.1016/j.nuclphysb.2008.01.002 [arXiv:0709.2899 [hep-th]].
- [94] D. Marolf, I. A. Morrison and M. Srednicki, “Perturbative S-matrix for massive scalar fields in global de Sitter space,” *Class. Quant. Grav.* **30**, 155023 (2013) doi:10.1088/0264-9381/30/15/155023 [arXiv:1209.6039 [hep-th]].
- [95] G. Narain, “Green’s function of the Vector fields on DeSitter Background,” arXiv:1408.6193 [gr-qc].
- [96] E. T. Akhmedov, “Lecture notes on interacting quantum fields in de Sitter space,” *Int. J. Mod. Phys. D* **23**, 1430001 (2014) doi:10.1142/S0218271814300018 [arXiv:1309.2557 [hep-th]].
- [97] M. Maggiore and M. Mancarella, “Nonlocal gravity and dark energy,” *Phys. Rev. D* **90**, no. 2, 023005 (2014) doi:10.1103/PhysRevD.90.023005 [arXiv:1402.0448 [hep-th]].
- [98] M. Maggiore, “Nonlocal Infrared Modifications of Gravity. A Review,” arXiv:1606.08784 [hep-th].
- [99] T. Appelquist and J. Carazzone, “Infrared Singularities and Massive Fields,” *Phys. Rev. D* **11**, 2856 (1975). doi:10.1103/PhysRevD.11.2856